UCRL- 97501
PREPRINT

SHALLOW DRILLING IN THE SALTON SEA REGION THE THERMAL ANOMALY

R. L. Newmark
P. W. Kasameyer
L. W. Younker

This paper was prepared for submittal to
The Journal of Geophysical Research

September 1987

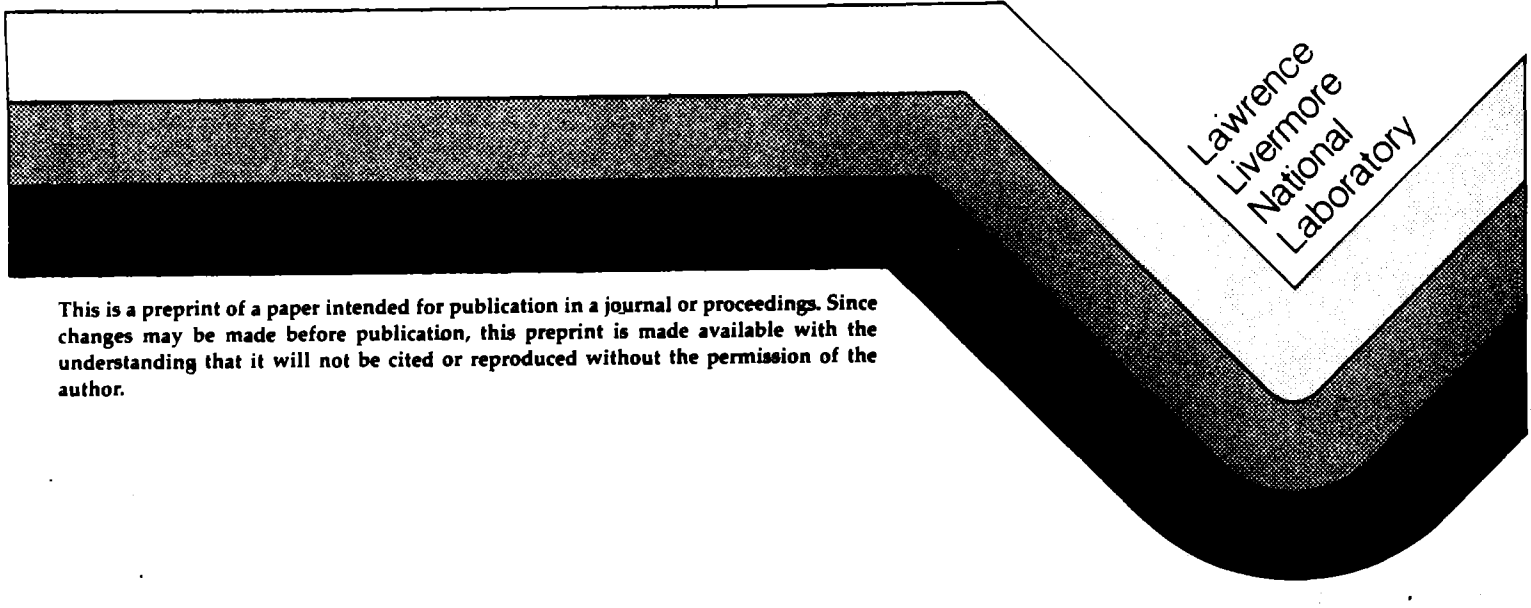

DISCLAIMER

SHALLOW DRILLING IN THE SALTON SEA REGION

THE THERMAL ANOMALY

Robin L. Newmark
Paul W. Kasameyer
Leland W. Younker

Earth Sciences Department
Lawrence Livermore National Laboratory
University of California
Livermore, California 94550
September 9, 1987

To be submitted to the Journal of Geophysical Research

ABSTRACT

During two shallow thermal drilling programs, thermal measurements were obtained in 56 shallow (76.2 m) and one intermediate (457.3 m) depth holes located both onshore and offshore along the southern margin of the Salton Sea in the Imperial Valley, California. These data complete the surficial coverage of the thermal anomaly, revealing the shape and lateral extent of the hydrothermal system. The thermal data show the region of high thermal gradients to extend only a short distance offshore to the north of the Quaternary volcanic domes which are exposed along the southern shore of the Salton Sea. The thermal anomaly has an arcuate shape, about 4 km wide and 12 km long. Across the center of the anomaly, the transition zone between locations exhibiting high thermal gradients and those exhibiting regional thermal gradients is quite narrow. Thermal gradients rise from near regional (0.09°C/m) to extreme (0.83 °C/m) in only 2.4 km. The heat flow in the central part of the anomaly is >600 mW/m^2 and in some areas exceeds 1200 mW/m^2. The shape of the thermal anomaly is asymmetric with respect to the line of volcanoes previously thought to represent the center of the field, with its center line offset south of the volcanic buttes. There is no broad thermal anomaly associated with the magnetic high that extends offshore to the northeast from the volcanic domes. These observations of the thermal anomaly provide important constraints for models of the circulation of the hydrothermal system. Thermal budgets based on a simple model for this hydrothermal system indicate that the heat influx rate for local "hot spots" in the region may be large enough to account for the rate of heat flux from the entire Salton Trough.

INTRODUCTION

The Salton Trough is a sediment-filled rift zone resulting from the oblique motion of the North American and Pacific tectonic plates over the last 4–5 my. It represents the transition between oceanic spreading in the Gulf of California to the south and the San Andreas continental transform fault system to the north (Elders et al., 1972) (Fig. 1). The thermal and structural processes that formed the Salton Trough were initiated when the East Pacific Rise intersected the North American plate margin, about 30 my ago (Blake et al., 1978). Since that time, the northward migration of the Mendocino triple junction and the southward migration of the Rivera triple junction marked the termination of subduction and the initiation of transform shear over a broad region (Atwater, 1970). This shear eventually produced the system of offset strike slip faults observed in the Trough. At present, the relative plate motion takes place primarily along transform faults such as the Imperial and San Andreas faults, with local zones of extension occurring wherever the faults are offset in a right-lateral sense, allowing magmatic intrusions to "leak" into the crust. These intrusions provide heat sources to drive hydrothermal activity. Several small Quaternary volcanic domes (Fig. 2) on the southeastern shore of the Salton Sea are direct evidence of the location of one of these "leaks".

The Salton Trough is a region of high heat flow. Heat flow measurements in the U.S. portion of the trough are above 100 mW/m^2 (Lachenbruch et al., 1985), more than twice the worldwide average. In addition, a number of small areas have especially high heat flow, >200 mW/m^2. These areas of hydrothermal circulation represent some of the largest and most accessible geothermal areas in North America, one of which is the Salton Sea Geothermal Field (SSGF).

The Salton Sea Geothermal Field has been extensively studied through regional geophysical surveys as well as shallow and deep drilling in the region southeast of the volcanic domes (e.g. Helgeson, 1968; Younker et al., 1982; Elders and Cohen, 1983). A wedge-shaped zone of seismicity called the Brawley Seismic zone coincides closely with the northern segment of the Imperial fault and extends northward through Obsidian Buttes at the southeastern end of the Salton Sea towards the southern tip of the Banning-Mission Creek branch of the San Andreas fault, in a diffuse pattern nearly coincident with the inferred location of the Brawley fault (Hill et al., 1975; Fuis et al., 1982, 1984). This is generally considered to be a spreading center in the form of a pull-apart basin. A local gravity maximum is centered over part of the geothermal field (Biehler, 1971). This anomaly has been attributed to either an increase in density of the sediments resulting from hydrothermal alteration, or the intrusion of dikes and sills into the sedimentary section, or a combination of these factors (Elders et al., 1972) (Fig. 3). A pronounced magnetic anomaly appears in Kelley and Soske's (1936) and Griscom and Muffler's (1971) magnetic surveys (Fig. 3). The magnetic anomaly is centered over the volcanic domes and extends offshore, into the Salton Sea along the zone in which seismicity has been detected at a slight angle to the extension of the gravity anomaly. Two elliptical northeast-trending anomalies are superimposed on the main trend, one over the volcanic domes and the other about 8 km offshore. The main magnetic anomaly has been interpreted to be due to the presence of intrusive rocks at depths greater than 2 km and the smaller, elliptical anomalies a result of dikes and sills at depths of about 1 km (Griscom and Muffler, 1971). A shallow heat flow survey utilizing a 2 m lance conducted in 1977 indicated extremely high thermal gradients in the vicinity of the offshore ellipsoidal magnetic high (Wilde, pers. comm.).

Two features of the temperature field in the southeastern part of the SSGF put strong constraints on models of the hydrothermal system (Younker et al., 1982) (Fig. 2). First, uniform, steady-state heat flow is observed in a 500 m thick thermal cap over a circular area about 30–40 km^2. Second, at the margin of the field, a narrow transition region, with a low near-surface gradient and an increasing gradient at greater depths, separates the high temperature resource from areas of normal gradient. A simple conceptual model of flow in the sampled portions of the field has been developed using these constraints (Kasameyer et al., 1984). Horizontal flow outward from a heat source located near the volcanic domes produces thermal fields which match the above observations. The model is simple enough that analytical results can be evaluated for a broad range of parameters in order to place bounds on characteristics of the hydrothermal system, such as its age and mass flow rates.

There were many unknowns about the field when this model was developed. The major uncertainty results because thermal gradients were measured only in part of the anomaly and none of the high heat flow contours were closed (Fig. 2).

Regional geophysics including the seismicity, gravity and magnetic studies mentioned above suggest that the "pull apart" zones extends under the Salton Sea. Very shallow temperature probes (Lee and Cohen, 1979) also suggest that the hydrothermal system similarly extends under the sea. Assuming symmetric flow patterns around the domes, we anticipated that an area of high (4 to 5 times normal) and uniform heat flow would be found offshore, and it could be detected and delineated by relatively shallow heat flow measurements in the conductive thermal cap. This paper describes the results of two shallow thermal surveys that complete coverage around the edges of the SSGF and into the previously unexplored area beneath the Salton Sea.

In the spring and summer of 1982, Kennecott-Bear Creek Mining Company (K-BCM) conducted a shallow drilling program to investigate the extent of the thermal anomaly along the southern shore of the Salton Sea. The temperature data and cuttings descriptions were released by K-BCM as part of their participation in the U.S. Department of Energy's Salton Sea Scientific Drilling Program. These data indicated that the thermal anomaly could be traced offshore and that the transition zone from areas exhibiting thermal gradients similar to those throughout the Trough to those exhibiting high thermal gradients is relatively narrow.

During the fall of 1985, the Lawrence Livermore National Laboratory and Sandia National Laboratories (LLNL-SNL) cooperated in drilling a series of shallow (80 m) holes for thermal studies in the southern Salton Sea (Newmark et al., 1986). The intent was to complete the surficial coverage of the thermal anomaly offshore in the region north of the line of exposed Quaternary volcanoes thought to represent the center of the thermal anomaly. These surveys have produced data that significantly change our view of the hydrothermal system at the Salton Sea.

METHODS AND INSTRUMENTATION

Drilling

During the months of May through August, 1982, Kennecott-Bear Creek Mining Company (K-BCM) drilled 41 holes both onshore and offshore along the southeastern and southwestern margins of the Salton Sea. The drilling sites were located using a hydrographic sextant. Offshore sites were located by 'shooting' the angles to existing sites and buoyed for ready identification. Hole locations are known to be within 15 m. Forty holes were drilled to 80 m with hole diameters ranging from 12.07-12.70 cm. A single hole (P6-4) was drilled 457.3 m onshore in the southwestern part of the Salton Sea Geothermal Field. This hole had a three-tier casing plan, ranging from 24.45-6.03 cm. The holes were drilled with a small truck-mounted rotary rig. Water was used as the drilling fluid; fresh for the onshore holes, sea water in a closed system for the offshore holes. Small amounts (a few kg) of drilling gel were added as needed. Drilling was relatively rapid, generally taking from 1-4 hours for the shallow holes. For those holes drilled offshore, the rig was set on a floating barge. Hydraulically-activated legs were driven into the lake bed in order to stabilize the drilling platform. The holes were cased with 2.5 cm diameter PVC pipe which was filled with fresh water (to reduce corrosion of the temperature logging equipment) and sealed at the bottom against infiltration of formation or surface fluids. Some of the holes drilled in May and July, 1982 (P1-19, P1-20, P2-11, P2-13, and P2-14), were backfilled with cuttings from the hole. The holes drilled after May were cemented through the drill pipe with 15 lb Class 'C' cement with returns to the surface. Pumping continued as the drill pipe was pulled to ensure that the hole was filled to the surface. The conductor pipe was then hammered back and stripped over the PVC pipe. The PVC pipe was left standing about 0.61 m above the surrounding area level (land or sea) for temperature logging. For the offshore holes, the PVC pipe was

also buoyed to minimize navigational hazards. Table I lists the hole locations, the date drilled and the date on which the last temperature log was run in each hole for all but two of these holes. One (P1-3) was lost during early data collection and another (P2-11) was redrilled (P2-11A). The holes were abandoned by the end of 1982.

In November and December, 1985, LLNL-SNL drilled nineteen additional holes 80 m below lake level offshore in the region north and west of the volcanic domes that lie along the southern shore of the Salton Sea. These drilling sites were located using a Motorola Miniranger* system, with an accuracy of about 2 m on the surface; in a maximum water depth of 18 m, buoy setting is known within 15 m. Each site was buoyed for ready identification. The holes were drilled with a truck-mounted rig set on a floating barge nearly identical to the K-BCM's offshore program (Fig. 4), using sea water in the circulation system. Drilling took an average of 2 hours. Lost circulation was not unusual, and it resulted in some holes, such as RDO-7Y, 6U, and 6Y) being shorter than planned. The holes were then cased with one inch diameter PVC pipe, filled with sea water and sealed at the bottom against infiltration of formation or surface fluids. Unlike the K-BCM program, high-temperature PVC (CPVC schedule 40) was used for casing the lower 30.5 m for most holes, to prevent closing and buckling of the PVC due to exposure to high temperatures over the following months. A 45.7 m stinger pipe was set along side the PVC and class 'G' cement was pumped through it to cement the casing. Pumping continued as the stinger was withdrawn to ensure that the hole was filled to the sea floor. The conductor was hammered back and stripped over the PVC, leaving 0.91 m of PVC above the sea surface. A heavy stand of conductor pipe (about 5.08 cm diameter) was pushed into the mud adjacent to each hole, and the PVC pipe was tethered to it to prevent the PVC from bending and sinking to the lake floor. The PVC was buoyed to minimize navagational hazards. Despite these precautions, some holes were lost before the logging phase of the project was completed, due to a combination of adverse weather, the weight

of rapid barnacle growth, and vandalism. One of the holes, RDO6D, was lost before any temperature logs were acquired in it. Lost circulation was a major problem during the drilling of many of the offshore holes. Table II lists the hole locations, the date drilled and the date on which the last temperature log was run in each hole. The LLNL–SNL holes were sealed and abandoned by the fall of 1986.

Lithology

During both drilling programs, cuttings samples were collected every 3 m when possible. The holes penetrate alluvial sediments composed predominently of clays, silts and sands. Quartz is the major silt and sand component. Volcanic glass occurs commonly in trace amounts, and is occasionally the primary component. Plant and rock fragments, gypsum, biotite, chlorite, muscovite and calcareous materials, including shell fragments, gastropods and ostracods, are common minor or trace components. These cuttings are available for use by others for additional scientific studies.

Temperature Logging

Temperatures were logged periodically in each hole in order to establish the thermal rebound history of the holes and to obtain equilibrium thermal profiles. The movement of the temperature sensor in the PVC pipe causes significant mixing of the water, disturbing the temperature profile. Therefore, all temperature profiles were logged going downhole. In the K–BCM program, two different systems were used for temperature logging: a Doric* temperature probe that utilizes a (100 Ω platinum RTD), and an Environ Lab* temperature probe, which also utilizes an RTD sensor. Temperatures were logged at stations every 3.05 m through the upper 18.3 m and every 1.5 m to the bottom of the hole, except for hole P6–4, which was logged every 6.1 m. The temperature profiles in this

report include interpolated temperature values at 4.6, 7.6, 10.7, 13.7 and 16.7 m. The thermisters were calibrated using ice baths and boiling water frequently during the logging periods. The response time for these instruments is on the order of one minute.

In the LLNL–SNL program, a temperature logging system developed by Sandia National Laboratories was used (R. Meyer, personal communication). The temperature sensor is a platinum resistance bulb (Weed* model 101–1A, 1000 Ω) having a published response time of 1 sec for 63.2% of a step change in water flowing at 0.91 m/sec. The rest of the logging tool was fabricated at Sandia National Laboratories of 0.29 cm OD brass tubing and a special fitting used to attach to the logging cable armor. The tool is packed with silicone grease to exclude water. Resistance of the RTD is measured using a Kiethley* model 195 autorange, remotely controllable multimeter. The resistance is determined using the 4 wire ohm mode every 0.03 m of travel. Temperature, depth and rate of travel are displayed to the operator. Time of day, temperature and depth are recorded on each of two computer discs and a continuous print of depth and temperature is produced. The logging cable, winch and depth measuring system are commercial units supplied by Mount Sopris*. Depth is measured using an encoder and counting system, and transmitted to the computer with a resolution of 0.03 m. Depth and rate are displayed to the operator. The logging cable is a 0.07 cm (3/16 in) OD 4 conductor cable about 305 m long. Each log was started from the same baseline zero point and ran continuously at a rate of 1.52 m/min to the bottom of the well. Trip error was measured at the end of each log and was on the order of 0.3–0.6 m. Logging speed was accurately controlled by a variable speed drive motor. All the final temperature log runs for the LLNL–SNL program were obtained with this system.

Figures 5 and 6 show the complete suite of temperature logs run in holes P1-14 and RDO7S, representing both drilling programs. Thermal rebound histories from the two programs differ in direction because the first was drilled with fluid significantly warmer than the shallow downhole temperatures, and the second with fluid that was cooler than the shallow downhole temperatures. Cement, whose heat of hydration also affects the thermal rebound, was emplaced in a slightly different manner in the two programs. Theory predicts that the temperature disturbance due to drilling alone (neglecting such factors as lost circulation heat of hydration of the cement) should decrease almost completely within a few days (e.g. Jaeger, 1965). Temperatures recorded in the shallow programs reached near-equilibrium within the first few weeks after drilling.

Hole P1-14 was drilled onshore during the K-BCM survey. The early temperature profiles are much higher than the equilibrium temperatures as the drilling fluid was relatively hot. (The water used as drilling fluid was trucked to the drilling location in tanks. Exposure to the high summer temperatures heated the drilling fluid.) In addition, the cement emplaced through the drillpipe provided a source of heat surrounding the PVC over the entire depth of the hole as it set up. The greater portion of the temperature disturbance subsided within the first few weeks after drilling. Locally high temperatures indicate zones of invasion of drilling fluid into the formation, which occurs in zones of relatively high permeability, for example, near 30 and 60 m. Such zones may have required a larger volume of cement, resulting in additional heat production.

Hole RDO7S was drilled in 1985 as part of the LLNL-SNL survey. This program was drilled in the winter, and the drilling fluid was much cooler than the downhole temperatures. Therefore, the early, disturbed temperature profiles show lower temperatures than the final ones. As the cement was emplaced no deeper than 45.7 m

from a stinger pipe alongside the casing, the lowermost 30.5 m of these holes were unaffected by the heat of hydration of the cement. The thermal profiles from the LLNL–SNL program rebound more rapidly to thermal equilibrium than the holes drilled during the K–BCM survey. The main differences between the programs are the time of year during which drilling and subsequent logging took place and the manner and depth of cement emplacement.

The final temperature logs for each hole are shown in Figures 7–10. In all cases, the zero depth for the temperature profiles lies within about 1.0 m above lake level (0 to $\pm$ 1 m) for those holes drilled offshore, or from the well top (within 1.0 m of ground level) for those drilled onshore. Lake level is 70 m below sea level. Zero depth is assumed to be constant with respect to sea level for all holes. The very gradual relief found nearshore (the vertical gradient is 1 in 1000) makes the assumption of no elevation change between holes a reasonable one.

Most of the holes exhibit fairly linear thermal profiles, indicative of conductive heat transfer. Changes in the thermal gradient with depth in most cases can be related to changes in the primary lithology, indicating conductive cooling. For example, hole RDO6N (Fig. 9) first penetrated about 45 m of predominently clay, then encountered a mixture of silt, sand and volcanic glass. The thermal gradient in the upper part of the hole is fairly constant and significantly higher than that below about 45 m, where it changes from about 0.68°C/m to about 0.44°C/m. This is a direct response to the change in primary lithology. The upper 39.6 m of hole P3–17 (Fig. 8) were also drilled into clay, the lower part of the hole penetrating sand. There is a distinct break in the thermal gradient at about 40 m, with a higher gradient in the upper portion, a lower gradient in the lower part of the hole. Applying reasonable values of thermal conductivity for each dominent lithology results in a constant heat flux through the formation, as will be discussed later in this paper.

Holes P2-6, P2-9, P2-10, P2-13 and RDO7A (Fig. 10) all exhibit nonlinear thermal profiles indicative of significant nonconductive or non-steady state heat transfer. These holes are located in the vicinity of the Imperial Carbon Dioxide Field, near the southeasternmost corner of the Salton Sea, itself suggestive of shallow circulation. Hole RDO7A lies within a few tens of meters from a series of active mud pots which are proof of shallow circulation. Other evidence of shallow circulation in the area are the nonlinear temperature profile in the upper few tens of meters in the Salton Sea Scientific Drilling Project (SSSDP) deep hole (Sass et al., 1987) and the presence of several mud volcanoes which occur a few hundred meters away from hole RDO7A onshore in a southeasterly direction, within sight of the SSSDP (Fig. 11).

The lower section of hole RDO6U (Fig. 8) below about 46 m shows an actual decrease in temperature with depth. Below 46 m, the hole penetrated volcanic glass before circulation was lost over the lowermost 18 m. This hole lies along the northwesterly line of features which show evidence of shallow circulation. Although the lowermost part of the hole indicates some circulation, probably lateral flow in the zone of highly permeable volcanic glass and sand, the upper section of the final thermal profile seems undisturbed, indicating a constant thermal gradient. Therefore, the thermal gradient at this location is included in Table II.

Thermal Conductivity

Thermal conductivity measurements were made on four cores, representing the bottom 1 m of holes RDO6T, RDO6Z, RDO7A and RDO7B using a needle probe system (Von Herzen and Maxwell, 1959) provided by Dr. Lee of University of California, Riverside. Thirteen of the measurements were made at either end of the solid core barrels. Five measurements were made at 7.6 cm intervals along the core from RDO6T

after drilling a series of small holes in the barrel for the probe to pass through. These eighteen measurements ranged in value from 0.89W/mK for a sandy clay to 3.23W/mK for a relatively dry, silty sand. The mean thermal conductivity of these measurements is 1.49W/mK. Figure 12 shows values obtained along the core from hole RDO6T, plotted versus depth in the core. These values show a 40% variation in thermal conductivity over only 30.5 cm. The wide range in thermal conductivities is a direct result of the changing lithology downhole. The coring process most certainly affects the water content of the cores, an effect for which we are unable to provide a correction. In addition, the measurements were made on both extruded and unextruded cores, which would also be expected to result in a difference in water content. The importance of these thermal conductivity measurements is in documenting the wide range of values possible in these sediments, rather than in defining a detailed conductivity profile for these few sites.

Preliminary results of laboratory measurements of thermal conductivity of drill cuttings by Lee and others at U. C. Riverside (Lee et al., 1986, and personal comm.) indicate a bimodal distribution of values, with the higher mode (1.9W/mK) corresponding to silty sand and the lower mode (1.0 W/mK) to silty clay. Comparison of the early temperature profiles and the preliminary thermal conductivity values reveals a trend toward higher thermal conductivity in zones of early temperature disturbance. This supports the theory that early disturbance in the temperature profiles is indicative of relatively high-permeability sandy material. Figure 13 illustrates this phenomena. The early temperature profile of hole RDO6N shows a few small zones of lower, disturbed temperature. Through the upper 20 m, the thermal gradient appears relatively stable, and the conductivity values average about 1.0 W/mK, indicative of the dominent clay content. At about 26 m, a local low in the temperature profile indicates thermal disturbance. This is accompanied by an increase in the thermal conductivity to almost 1.7 W/mK. This zone contains about 90% silt. Between about 35 and 50 m, the stable

thermal gradient is re-established, and the thermal conductivity remains low. Thermal disturbances from 53-61 m and at about 75 m are similarly accompanied by increased thermal conductivites. Cuttings from these zones show an increase in silt content. Unfortunately, the sample frequency is not sufficient to apply these values of thermal conductivity directly to the thermal gradients measurered downhole for the calculation of heat flow.

In measuring the thermal conductivity of these relatively unconsolidated sediments, the porosity of the sample is an important factor. The larger the clay fraction, the smaller the potential errors in reconstituting the sample's original fluid content. Therefore, for calculation of heat flow, it is preferable to obtain the thermal gradient over zones in which the primary lithology is clay, whose thermal conductivity is better known.

RESULTS

Thermal Gradients

Vertical thermal gradients were calculated over the lower 46 m of each final temperature profile. Although most of the LLNL–SNL program holes were logged up to 5 months after drilling, during which time a stable thermal gradient was established, many of them had not reached thermal equilibrium. For each of the LLNL–SNL holes, we first evaluated the equilibrium formation temperature using the method of Barelli and Palama (1981). This method uses the temperature rebound history in the holes after a finite drilling disturbance to estimate the formation equilibrium temperature at each depth. Thermal gradients were calculated over the lower 46 m of the predicted equilibrium temperature profile using a least squares fit. Although this method does not account for the presence (and heat of hydration) of the cement, since the cement only extended to 46 m, and the thermal gradients were calculated below 30 m, the presence of the cement does not significantly affect our results. Ninety percent of the thermal gradients calculated over the lower 46 m of the last temperature log for each hole were within 5% of those obtained from the predicted equilibrium temperatures, showing that a stable thermal gradient had been established even if the individual equilibrium temperatures had not yet been reached. The results are presented in Table II and Fig. 14. The thermal gradient values are accurate to within $\pm$6% (95% confidence limits).

We were unable to apply the Barelli and Palama technique to the K–BCM program holes for the following reasons: 1) cementing the entire length of the hole resulted in an early-time source of heat, which affected the thermal rebound history for each hole in a manner for which the Barelli and Palama method cannot correct, 2) temperatures were obtained in a very coarse spacing, making it difficult to clearly define the temperature

rebound in zones of early temperature disturbance, and 3) most of the holes were not logged frequently enough to establish the rebound history. Vertical thermal gradients for the K-BCM program holes are calculated over the lower 46 m using a least squares fit, with accuracies within ± 6% (95% confidence limits). The results are presented in Table I and Fig. 14.

The two new datasets were combined with previously published data and new temperatures measured in State 2-14 (Sass et al., 1987) to produce maps of thermal gradient and heat flow in the conductive cap. The deep well data came from two papers. For 11 deep holes in the Salton Sea Geothermal Field, we used average thermal gradients in the cap, estimated by Younker et al. (1982), using temperatures from a number of sources. We also estimated gradients from temperature data reported by Muramoto and Elders (1984), for four deep wells with nearly uniform gradients in the Westmorland and Niland areas. Shallow gradient values from Sass et al. (1984), were retrieved from his heat flow map by dividing out his assumed thermal conductivity , 1.88 W/mK. Fourteen of 15 data points were eliminated as they appear to be based on the deep hole measurements used by Younker et al. (1982). All measurements in these datasets are based on observations below 30m in boreholes, and therefore require no corrections for annual temperature cycles.

These data allow us to complete the surficial coverage of thermal data in the area surrounding the Salton Sea Geothermal Field. The dominant features of the contour map (Fig. 14) are two extremely high temperature zones, or bullseyes, which we call the Mullet Island anomaly, located at the northeast corner of the geothermal field, and the Kornbloom Road anomaly, located to the southwest. The existence of high temperatures at Mullet Island was expected because of observed mud return temperatures in well Pioneer Development Corporation #1, drilled on the island in 1927. Mud was heated to 65 °C when the hole depth was 45 m indicating a high thermal gradient, perhaps above 1.0

°C/m (State Division of Oil and Gas, personal communication). The Kornbloom Road Anomaly was not reported before this survey. The axial portion of the thermal anomaly is arcuate, about 4 km wide and about 12 km long. It extends only a short distance offshore, primarily in the northern and southern edges of the geothermal field. The axial anomaly is not centered on the chain of volcanic buttes. Its northwestern boundary follows an arc roughly coincident with the pattern of the buttes. The high temperature region in the south extends beyond the magnetic anomaly, in contrast to the northeastern region where the thermal and magnetic anomalies appear to be closely correlated. There is no evidence of a broad local thermal anomaly associated with the offshore magnetic high, but because of our loss of hole 6D before temperatures could be measured, coverage of that anomaly is poor.

Heat Flow

In previous studies (e.g. Sass et al., 1984), an average value of thermal conductivity for the region (e.g. 1.88 W/mK) was applied to the thermal gradient for each hole. Preliminary results indicate that the thermal conductivities may vary by a factor of two (T. C. Lee, unpublished data), which could result in a factor of two difference in the calculated heat flow. In this study, the detailed lithologic descriptions allow us to refine the estimate of thermal conductivity according to the dominant lithology over an interval.

Heat flow values from the shallow holes are calculated using the average thermal conductivity measured for the primary lithology in the interval over which the thermal gradient is measured. These values of thermal conductivity are averages of the preliminary thermal conductivities measured on the cuttings samples from the LLNL-SNL holes by Lee and others (T. C. Lee, unpublished data) and are as follows: clay = 1.0 W/mK, clay with some silt = 1.3 W/mK, silty clay = 1.4 W/mK, clayey silt = 1.7 W/mK, silt = 1.8

W/mK, and sand or sandy silt = 1.9 W/mK. These values are accurate to within about 17%. Whenever possible, heat flow was calculated over intervals whose primary lithology is clay, whose measured thermal conductivity is less sensitive to the proper reconstitution of the water content. In holes in which there is more than one interval with a dominant lithology, the heat flow calculations using these average values agree closely. The results are listed in Tables I and II and plotted in Figure 15. The heat flow values are accurate to within ± 12% (95% confidence limits in thermal gradients and ± 0.10W/mK in thermal conductivity).

There is some evidence that the assumption of conductive cooling in the upper cap is not valid throughout the field. A few holes that exhibit nonlinear temperature profiles uncorelated with changes in lithology lie along the northeastern edge of the field, located in the vicinity of the Imperial CO_2 field. As discussed in the section on temperature logging, there are a number of offshore boiling mud pots and active mud volcanoes onshore (Fig. 11) which lie along a northwesterly linear trend running through the Mullet Island Anomaly. These features are evidence of circulation, probably associated with faulting, which may mean that the Mullet Island bullseye results mainly from leakage. There is no such evidence of shallow circulation or leakage in the vicinity of the southern bullseye.

The heat flow contours follow roughly the same pattern as the gradient map. Lachenbruch et al. (1985) showed that the Salton Trough has a background heat flux between 100 and 200 mW/m^2, with a reduced heat flow for the Imperial Valley of about 125 mW/m^2. The heat flux in the central part of the Salton Sea anomaly is generally in excess of 500 mW/m^2, and in the Mullet Island and Kornbloom Road bullseyes exceeds 1200 mW/m^2. The center of the zone of highest heat flow follows an arc with about 8 km radius of curvature, centered NW of the domes.

Factors Affecting Thermal Gradients

Do our measured thermal gradients accurately represent the undisturbed gradients in the conductive zones of the Salton Sea Geothermal System? Topography, changes in climate, the occasional formation of lakes and incursions of the ocean into the Salton Trough all could disturb the shallow gradient. For our surveys, topographic effects are certainly small, and climate changes can be ignored, but the lakes, particularly occasional ones, can have effects on both onshore and offshore heat flow measurements in shallow holes. Detailed knowledge of the hydrologic and surface temperature histories, as well as erosional and depositional environments, are required for quantitative corrections for these effects. This is difficult in the case of the Salton Sea, as it has had a complex history, with numerous filling and evaporation cycles since the Pleistocene. For example, the present Salton Sea was created by accidental diversion of the Colorado River in 1905–1907. A lake preceding the present one filled in 1890 and became dry soon thereafter. In the late Pleistocene, Lake Cahuilla occupied an area several times larger than the present one. The present southern shoreline of the Salton Sea has moved over 1.6 km landward in the last decade alone. The general concordance of shallow surveys and temperatures from deep wells here and throughout the Imperial Valley suggests that these fluctuations in surface conditions have produced only insignificant perturbations in the gradients measured in shallow holes. However, we do observe a substantial change in the thermal gradient at the edge of the axial anomaly that is nearly coincident with the present shore of the lake. Is this rapid change merely an artifact of the present size of the lake? Lee and Cohen (1979) used conductive heat flow models to place limits on the perturbation of the thermal gradient by the Salton Sea. Following their analysis we estimate conductive effects of the lake, and also examine the possibility that downward infiltration of fluids has reduced the gradient. Our conclusion is that these effects are negligible, and the abrupt change in gradient is real.

The creation of a lake can impose an average surface temperature different from the mean annual temperature, disturbing the gradient at depth. Lee and Cohen (1979) estimated that the mean annual temperature at the bottom of the Salton Sea is 5.5 ^{o}C below the mean air temperature. We have used two approaches to evaluate the the effect of this instantaneous temperature change on our measurements.

Jaeger (1965), solved the one-dimensional, transient heat conduction equation for a step change in surface temperature of ΔT at t=0. He showed the disturbance in the surface gradient is given by $\Delta T/(\pi\alpha t)^{1/2}$. Using a diffusivity $\alpha = 3.78 \times 10^{-7}$ m^2/s (the mean value calculated by Lee and Cohen (1979) and 80 years for the age of the Salton Sea, we estimate that the offshore gradients could be artificially raised by 0.10 °C/m at the surface, and by 0.01°C/m at a depth of 30 m, below which the thermal gradients were calculated. As most of the southern part of the lake is less than 6 m deep, the difference between the mean annual temperature of the lake and the ground surface is probably less, and thus this value is probably an upper limit for the surface disturbance. Lachenbruch (1957) used a two-dimensional solution to include the perturbation on the shore of the body of water. This effect, which is no larger than the one-dimensional value under the lake, can possibly be seen in the upper 20 m of some of our data near the sea. We conclude that this disturbance, about three times greater than the normal upper crustal gradient at the surface, would produce only a 1.0% increase in our gradients measured below 30 m depth.

Sedimentation can reduce the thermal gradient locally, and the magnitude of the effect on the surface heat flux depends on the rate and duration of sedimentation, as well as the thermal properties of the sediments. If the sediments were instantaneously dumped into the lake, the thermal blanketing effect would have reduced the steady gradient at the surface by a factor of $\mathrm{erfc}[d/2(\alpha t)^{1/2}]$ (Von Herzen and Uyeda, 1963). For sediment

thickness d of 1, 2, 4, and 8 m, the reduction is 1, 2, 4 and 7% of the steady gradient, respectively. In the southern part of the Salton Sea, dead trees mark fence lines of now-flooded farms, and telephone poles mark inundated roads. Although the thickness of the lake sediments deposited since 1905 vary from place to place, it is clear, from the surviving pre-1905 artifacts and the shallow probe penetrations of Lee and Cohen (1979), that the sediment thickness is no more than 4 m, and probably no more than 2-3 m in the vicinity of the LLNL-SNL and K-BCM programs. In the Brawley area, just south of the Salton Sea, sediments at about 25 m depth are about 1500 years old at most (Simms and Rymer, pers. comm.), indicating an average sedimentation rate of about 1.7 cm/yr. If a 3 m layer of sediments were deposited at a constant rate over the past 80 years (a rate of 3.75 cm/yr, or twice that observed just south of the lake), the reduction in surface thermal gradient would be about 11% (Jaeger, 1965). This reduction decreases to 0.02°C/m at a depth of 30 m, below which the thermal gradients were calculated. Thus, the effect of sedimentation might reduce the observed gradient by no more than about 2%.

Infiltration can drastically decrease the thermal gradients beneath bodies of water, but its effects can be detected by curvature of the temperature profile. Bredehoeft and Papadopulos (1965) found a solution for steady-state, one-dimensional infiltration to depth L.

$$T(z) = T_0 + g_0 L \frac{\exp(\beta z/L) - 1}{\exp(\beta) - 1}$$

where $\beta = VL/\alpha$, V is the Darcy velocity of the infiltrating water (positive downward) and g_0 is the undisturbed gradient over the depth range 0 to L. We can use our observation that over the 80 m depth of our wells, represented by ΔZ, the observed gradient is constant to within about 10%, (i.e. $\Delta g/g$ is less than 0.10) to put an upper bound on the infiltration velocity.

$$g(z) = \frac{dT}{dZ} = g_0 \beta \frac{\exp(\beta z/L)}{\exp(\beta) - 1}$$

$$\frac{\Delta g}{g} = \frac{1}{g}\frac{dg(z)}{dg}\Delta Z = \beta \Delta Z/L < 0.1$$

Substituting for β, $V < 0.1\alpha/\Delta Z = 0.015$ m/year for the diffusivity used above. Any higher velocity would produce detectable curvature on our profiles. Even such a low infiltration velocity could reduce the observed gradients significantly, depending on the depth of infiltration. For L = 500 m, a typical depth of the bottom of the thermal cap, the gradient is reduced by 30%, and for L = 2000 m, the gradient is reduced by a factor of four. However, in the short time since the Salton Sea formed in 1905–1907, infiltration at this rate could not penetrate far into the sediments. The penetration depth of the infiltrating water is given by the ratio of the Darcy velocity to the porosity, resulting in <12 m of infiltration in 80 years if the porosity is 10%, or only 2.4 m if the porosity is 50%. We conclude that recent infiltration has not reduced the gradients measured below 30 m. Without detailed knowledge of previous lake shorelines and lifetimes, it is not possible to determine the cumulative effect of infiltration. However, to cause the observed localized change in gradient, we would require that short-lived lakes had their shorelines in the same place for thousands of years, an unlikely possibility in this area with no topographic relief.

At the depth interval over which the thermal gradients were calculated, all of these effects are relatively small. The reduction in thermal gradient due to sedimentation is potentially the largest effect that may influence the thermal gradients obtained in the shallow holes. This is partly offset by the potential increase in thermal gradient due to the creation of the Salton Sea. At most, the offshore thermal gradients are as much as about 0.01°C/m higher than measured. The close agreement between the thermal gradients and heat flow determined in holes located directly offshore and those determined for nearby holes located directly onshore on the northeast and southwest edges of the thermal anomaly supports the conclusion that the thermal gradients are not substantially affected by the presence of the lake.

DISCUSSION

Nature of the Salton Sea Geothermal Anomaly

The Salton Sea Geothermal Field is characterized by three nested thermal features superimposed on the regional Salton Trough heat flux, shown schematically in Fig. 16. A broad region of elevated conductive heat flow surrounds a high temperature axial anomaly. This broad anomaly is characterized by constant temperature gradients on the order of .1°C/m persisting to depths of over 2500 meters and producing 250°C bottom hole temperatures. The axial anomaly occupies an area of 30-40 km^2 asymmetrically distributed about the volcanic buttes. Very high (0.4°C/m) near-surface gradients are observed through a thermal conductive cap to depths of approximately 500m. A nearly isothermal zone underlies this conductive zone to depths greater than 2500 meters. Bottom hole temperatures on the order of 350°C are observed in this area. The boundary between the axial anomaly and the broad conductive anomaly is characterized by temperature gradients that increase with depth near the base of the thermal cap. Small intense thermal plumes, the Mullet Island anomaly and the Kornbloom Road anomaly, with shallow temperature gradients as high as 0.8°C/m are superimposed on the main axial hydrothermal system reflecting shallow fluid movement. The vertical extent of this region of very high gradients is unknown but plausible temperature arguments limit these features to be less than a few hundred meters thick.

The nature of the axial anomaly is illustrated in the anomalous temperature cross-sections shown in Fig. 17a and b. Assuming the axial anomaly is superimposed on the broad anomaly, a constant gradient (0.10°C/m) profile has been subtracted from all temperatures, leaving only the excess due to the axial anomaly. Section $A-A^1$ crosses the axis from NW to SE, and shows the broad uniform temperature zone across the anomaly

and the abrupt drop-off at its edges, particularly the SE edge. Section B-B[1] crosses the same anomaly nearly perpendicular to its easternmost edge. Here the outer boundary is much broader. Most of the anomaly is on one side of the line of volcanoes. The anomalous temperature contours close to the SE, but the absence of deep data under the Salton Sea leaves uncertainty about whether the NW boundary is similar to the SE.

Conceptual View of the Salton Sea Geothermal Anomaly

Several factors control the size, shape and characteristics of thermal anomalies in the earth's crust. These factors include the location and characteristics of the heat source, heat transfer mechanisms (including preferential flow pathways), pre-existing thermal structure, and time since the inception of the system. Previous studies have provided constraints on these factors. A conceptual model was developed involving a localized heat source near the volcanic buttes and horizontal fluid flow to the southeast (Younker et al., 1982). Alternative flow pathways to the northwest have been proposed (Riney et al., 1977), but they are inconsistent with the data from the field (Kasameyer et al., 1984). Simple calculations based on the rapid spatial change in surface gradient between the main hydrothermal system and the conductive region indicated that the thermal anomaly, represented by the main hydrothermal system, is quite young (3,000 - 20,000 years).

The shallow temperature surveys have provided the basis for refining this conceptual view of the system. The northwest boundary of the main hydrothermal system has been described, and the existence of the local plumes has been documented. These additional observations further constrain plausible models for the field. As a result of the surveys, we now have a good idea of the plan view of the region of elevated heat flow, both its area and shape. Because of the existence of the conductive thermal cap, we can also make inferences about the deeper thermal structure.

A comparison of the shape of the thermal anomaly with the pattern of the geophysical anomalies and the location of the volcanic buttes leads to a refined conceptual model of the field. A broad area of high conductance extends along the axis of the valley away from the volcanic buttes (Younker et al., 1982). This resistivity anomaly probably reflects the boundary of the saline brine, and lends support to a model in which hot fluid is channeled to the southeast in a permeable aquifer beneath the thermal cap. The gravity anomaly is also offset slightly to the SE from the buttes (Fig. 3) reflecting the region of sediments which have been altered by the interaction with the hot brine. The coincidence of the pattern of volcanic buttes and the shape of the elliptical magnetic anomaly (Fig. 3) indicates that the buttes likely overlie a deeper magmatic heat source in the form of distributed dikes and sills. The similarity of the arcuate NW boundary of the thermal anomaly to the spatial pattern of the volcanic buttes suggests that this region may also mark the location of the upwelling of the hot fluids (Fig. 14). The narrow transition between the region of high gradients in the field and the lower values to the southeast (Fig. 14, 17a) provides further support for the lateral flow system. The broader transition on profile B–B^1 (Fig. 17b) suggests that other mechanisms are important in that area. The position of flow upwelling is not well constrained, and it could be located somewhat to the SE of the volcanic buttes. There is no evidence for flow of hot fluids past the position of the volcanics to the northwest.

Factors Controlling the Nature of the Salton Sea Geothermal Anomaly

The arcuate geometry of the domes, and the position of inferred fluid upwelling may be controlled by the complex stress regime in the pull apart region between the San Andreas and Brawley fault zones. Crowell (1974) has described and qualitatively analyzed features associated with the development of pull-apart basins of this type. Rodgers (1980) and Segall and Pollard (1980) developed mathematical models to describe the

patterns of basin formation and faulting related to the evolution of pull-apart basins. Segall and Pollard (1980) concluded that dike intrusion would be favored in the region of reduced mean stress between offset right lateral faults.

Major features applicable to the Salton Sea stress regime have been inferred from simple calculations in which the San Andreas and Brawley fault zones are modeled as elastic dislocation surfaces within a semi-infinite homogeneous elastic medium (Full, 1980). The calculations use the basic theory and equations derived and discussed by Chinnery (1961, 1963). Figure 18 shows Full's calculation of normal stress in the ground surface for two faults with geometry and characteristics broadly representative of the Banning-Mission Creek branch of the San Andreas fault and the Brawley fault. The results indicate the presence of a relative tensile region concentrated at the northwest end of the smaller and shallower Brawley fault and a smaller one at the southwest tip of the Banning-Mission Creek fault. The zone of maximum relative tension runs between the two faults describing an arc coincident with the arcuate pattern of the volcanic chain, and mirroring the northwest boundary of the thermal anomaly. Enhanced vertical permeability due to fracturing would be expected to facilitate localized upwelling of fluids in these regions. These areas would also mark the most likely locations for shallow intrusion of basaltic and rhyolitic dikes. The subsurface igneous activity in the region is evidenced by the discovery of altered basaltic and silicic dikes and sills in several of the geothermal wells in the field (Robinson et al., 1976; Herzig and Mehegan, 1986; Lilje and Mehegan, 1986).

Factors controlling the flow of hot fluids to the southeast are possibly related to primary depositional permeability in the sedimentary section, existence of flow barriers related to the emplacement of dikes, or regional fluid flow directions. The lithologic cap

has been shown to be thicker towards the Colorado River (the sediment source) to the southeast. The beds dip to the northwest. This configuration may provide preferential flow paths up-dip through the more permeable beds to the south, but prevent shallow circulation to the north. If this is the dominant effect, vigorous circulation may occur at greater depth in the region north of the volcanic chain. Alternatively, the sediments north of the volcanic line may, for some reason, be less permeable than those found in the center of the field to the southeast. A third possibility is that regional flow is directed southeast along the Salton Trough through the field. Rex (1983) has proposed such a model based on chemical arguments.

Thermal Regime of the Salton Sea Scientific Drilling Project Site, State 2-14

The above discussion provides a context within which to view the thermal regime of State 2-14, which is located on the edge of two of the nested thermal features in the field. First, it is on the boundary of the Mullet Island anomaly, and second, it is near the edge of the axial anomaly representing the main hydrothermal system. Sass et al., 1987 report that the State 2-14 has an unusually high near-surface gradient perhaps associated with the shallow thermal plume near Mullet Island. Below 150m the well has temperatures intermediate between wells in the central axial zone and wells in the broad conductive zone. There is, however, no evidence in section B-B^1 to suggest lateral flow of hot fluids away from the center of the field, such as is observed in the region between the axial anomaly and the conductive zone along the axis of the Trough to the south. This difference may reflect the effects of a fault barrier or lateral changes in the permeability of the sedimentary section.

One of the intriguing results of the SSSDP has been documentation of a retrograde thermal regime (Andes and McKibben, 1987; Sturtevant and Williams, 1987). Fluid

inclusion and pore fluid studies suggest that the upper 1 km of the well may have cooled by 40 - 100°C. If, as is suggested by Kasameyer and Hearst (1987), the portion of the broad thermal anomaly to the northeast of State 2-14 represents a cooling, earlier pulse of hydrothermal activity, then thermal profiles at State 2-14 may reflect transient cooling from this earlier activity.. The proximity of the Mullet Island thermal plume to the State 2-14 site can provide an alternative explanation for the observed retrograde thermal regime. Anomalously high heat flow is currently being pumped from the area due northwest of the SSSDP, drawing relatively cooler fluids in from the surrounding area. In this process heat to drive the plume may, in part, be coming from deeper, higher temperature regions surrounding the plumes. This presumably transient process superimposed on the main hydrothermal activity would be expected to produce localized regions of retrograde thermal activity.

Salton Sea Geothermal Field and Crustal Rifting in the Salton Trough

The processes of crustal extension and rifting in the Salton Trough may be viewed on many different scales (Fig. 19). On the smallest scale the thermal zones, each less than about 10 km wide, are believed to be the current locus of spreading (Elders et al., 1972). A pattern of modern intense seismicity suggests to others that a zone perhaps 30 km long is actively deforming in response to the crustal rifting process (Fuis et al., 1982, 1984). On an even larger scale regional heat flow considerations indicate that extension and basalt intrusion must occur throughout a diffuse zone of deformation 150 km long in order to be consistent with the observed crustal structure and appropriate strain rates (Lachenbruch et al.., 1985). Any model for crustal rifting in the Trough must reconcile observations on these diverse scales.

A critical issue to resolve is the relationship of the individual geothermal anomalies to the overall process of crustal rifting in the Trough. One view is that these systems

represent localized relatively unimportant near-surface perturbations of the regional rifting process, perhaps analogous to the high temperature plumes in the Salton Sea geothermal system. An alternative view is that these geothermal systems actually are the current locus of spreading in the Trough, reflecting regions of elevated mantle heat flux into the Trough.

An analysis of thermal budgets provides one means for linking the local systems with the regional rifting process. An important question to address is how large a contribution to the total heat flow comes from the local areas of high heat flow? Sass et al.'s (1984) area heat flow survey of the Imperial Valley indicates that the zones of anomalously high heat flow (the geothermal fields) representing 10% of the area, contribute only 25% of the total heat flow out of the valley. The local systems providing a relatively small portion of the heat flow out of the valley might, therefore, be relatively insignificant features in the context of the trough-wide rifting process.

Alternatively, if it can be shown that the geothermal fields are young and growing, they could conceivably still account for the heat input necessary to satisfy the thermal budget of the Trough. A critical question to resolve is, what is the rate of heat flow into these areas? If it is greater by a factor of 4 or more than the heat flow out, then the rate of heat flux into the small, hot zones is as large as all the heat flowing out of the Trough. Under this model there would be no anomalous heat transport into other areas of the trough, which must be cooling off from periods of earlier active heat input. Thus, by examining the ratio of heat flux out to heat accumulation rate, we can test whether it is possible that all the spreading and anomalous mantle heat flux takes place at these zones.

The heat flux into a geothermal system cannot be measured directly with near-surface observations. The conceptual model for the Salton Sea field does, however,

provide a basis for estimating the heat flux into that system. A simple lateral flow model can be used to model the transfer of hot fluids from the region of upwelling near the buttes, southeast in a reservoir beneath a conductive thermal cap. The model can be used to calculate temperature gradient profiles in the thermal cap for comparison with observations in the field (Kasameyer et al., 1984). In that paper it was shown that calculated temperature profiles are dependent upon the age of the system, the fluid residence time in the aquifer, and a parameter reflecting the ratio of the heat capacity thickness products of the saturated aquifer and cap rock. A recent re-evaluation of this model indicated that these parameters can be used to relate the heat input rate to the heat loss rate of the system.

Field observations, mostly notably the width of the transition zone between the expanding hydrothermal system and the conductive anomaly can, therefore, be used to estimate the rate of influx into the system. To fit the observations from the Salton Sea geothermal area, the ratio of heat flux into the system by advection to the rate of heat flux from the top of the system by conduction is somewhere between 2.8 and 10 (Kasameyer et al., 1984). Models with parameter values outside this range produce broader transition regions than those observed. If the predictions of this model are valid, and if other local hot spots are growing as rapidly as the Salton Sea Geothermal Field, then these small, ephemeral geothermal systems may account for the total heat flux from the entire Salton Trough.

Thus, the Salton Trough could represent a broad region that has undergone spatially variable pull-apart basin development and growth. Shallow hydrothermal systems in the pull-apart region between active strike slip faults are the near surface expression of the rifting process. Transfer of motion between adjacent fault zones and extension of fault traces in response to the southward passage of the Rivera triple would change the position with time of these zones of active spreading. From a thermal budget

viewpoint heat input to the Trough is localized in the regions of active pull-apart development. As the complex system of subparallel faults evolved, new pull-apart structures and zones of spreading developed. Total heat flow out of the Trough is a result of the transient cooling of the previously active spreading centers coupled with the heat flow from the current centers. Thus, relatively small ephemeral zones of intrusion can create a broad zone of high heat flow consistent with the model of Lachenbruch et al. (1985).

SUMMARY AND CONCLUSIONS

Two shallow thermal gradient surveys have bounded the spatial extent of the Salton Sea high temperature hydrothermal system and documented the presence of two superimposed shallow high temperature plumes. The Salton Sea field can now be characterized as a system of 4 nested thermal zones with each zone representing the dominance of different mechanisms of thermal transport. The largest zone covering most of the Imperial Valley has an anomalous high thermal gradient of about 0.07°C/m (Sass et al., 1984). At an intermediate scale, a broad zone with nearly conductive temperature profiles of .1°C/m surrounds the highest temperature hydrothermal system on at least 3 sides. The central part of the geothermal field is identified as a region of broad uniformly high near surface gradient (.4°C/m) and decreasing gradients at depth implying convective transport. Within this region two localized intense shallow zones with gradients as high as .8°C/m have been identified.

The characteristics of the thermal anomaly, coupled with the geophysical data from the area, provides the basis for developing a conceptual model for the Salton Sea system. Localized upwelling of hot fluids near the volcanic buttes is followed by horizontal flow to the southeast in a permeable aquifer beneath a thermal cap. The location of the region of upwelling is controlled by the complex stress regime in the pull apart region between the San Andreas and Brawley fault zones. The preferential flow pathways to the southeast likely reflect either primary permeability variations or interaction with the regional flow system.

A simple quantification of this conceptual model allows us to make inferences about the thermal budget of the Salton Sea field. Estimates of the total area of the field, heat flux out of the field, the thickness of the circulating zone, and the abruptness of the transition to the regional gradient are used to calculate the rate of heat flux into the

field. The results suggest that the Salton Sea field is young and growing. The best fit to the thermal data indicates that the ratio of the heat flux in to the heat flux out is between 2 and 8. A comparison of this value with regional heat flow constraints provides support for a model in which small ephemeral geothermal may account for total heat flux from the Salton Trough.

ACKNOWLEDGEMENTS

This work was supported by the Office of Energy Research, Division of Engineering and Geosciences, U. S. Department of Energy as part of the Continental Scientific Drilling Program. We thank George Kolstad, Jim Coleman, Dan Weill, and Ed Schreiber for their support for this project and the overall Department of Energy Continental Scientific Drilling Program. The Geoscience Research Drilling Office of Sandia National Laboratories, under the direction of Jim Dunn and Peter Lysne had complete responsibility for operations and logistical support for the project. We especially thank Peter Lysne for his enormous efforts and technical contributions. Bob Meyer and Ron Jacobson of Sandia designed the temperature logging system and fielded it under conditions that were often quite difficult. They are responsible for the high quality of the data.

This project would not have been possible without the support of the geothermal industrial community. Kennecott Geothermal, UNOCAL Geothermal, Trans-Pacific Geothermal, Inc., and I. Sheinbaum Co., Inc. all provided access to their lease holdings. We would like to thank Larry Grogan (Kennecott Corporation, Salt Lake City, Utah) and Pam Irvine (formerly of UNOCAL) for their enthusiastic support of the project, along with Ian Padden and his drilling and marine support crew for their hard work and efforts through what were often difficult and windy working conditions.

* Work performed under the auspices of the U.S. Department of Energy by Lawrence Livermore National Laboratory under Contract W-7405-Eng-48.

FIGURE CAPTIONS

Figure 1. Schematic structural relations in the Salton Trough adapted from Lachenbruch et al.. (1985). Stippled area represents extent of crystalline basement from Goddard (1965). Dots represent major geothermal areas. Abbreviations are S.S., Salton Sea; B, Brawley; E.M., East Mesa; H, Heber; C.P., Cerro Prieto; W, Wagner Basin. Squares indicate inferred zones of pull-apart spreading. Heavy arrows indicate relative plate motion.

Figure 2. The Salton Sea geothermal area. The dotted pattern shows the region in which previous studies have provided data used in modeling the system (Kasameyer et al., 1984). The four small stippled areas mark the locations of the Quaternary volcanoes. Temperature profiles from the central part of the geothermal field (A) show that this part of the field (A) is characterized by a broad region of moderately high uniform heat flow in the upper few hundred meters and a nearly isothermal zone at depth. The outer region (B) is characterized by relatively low heat flow and uniform thermal gradients. The narrow transition region between A and B is characterized by thermal profiles showing a relatively low heat flow near the surface, but the gradient increases with depth (C) (after Newmark et al., 1986). Diagonal lines mark the area investigated by the two shallow drilling programs presented in this paper.

Figure 3. Geophysical anomalies in the southern Salton Sea region (after Younker et al.., 1982). Dots mark the locations of the volcanic domes. A) Complete Bouguer gravity anomaly (after Biehler, 1971). B) Aeromagnetic anomaly (after Griscom and Muffler, 1971).

Figure 4. Drilling platform for the LLNL-SNL program. A truck-mounted rotary drill rig is anchored atop a barge. Three hydraulically-activated legs (shown in nearly full-up

position) were driven into the lake bed to stabilize the drilling platform. The SSSDP rig is visible in the distance.

Figure 5. Temperature profiles obtained in hole P1-14 ranging from 1 day to 82 days after drilling. Depth shown is depth below lake bottom. See text for discussion.

Figure 6. Temperature profiles obtained in hole RDO7S ranging from 1 hour to 62 days after drilling. Depth shown is depth below lake surface. See text for discussion.

Figure 7. A-D) Final temperature profiles for holes exhibiting generally low thermal gradients <0.20°C/m. For ease of presentation, the starting temperatures are offset by 20°C for all but the first profile displayed. Depth shown is depth below lake surface (offshore) or ground level (onshore). All logs project to a surface temperature of about 20°C. Holes drilled as part of the K-BCM program include interpolated values at 4.6, 7.6, 10.7, 13.7 and 16.7 m.

Figure 8. Final temperature profiles for holes exhibiting intermediate thermal gradients, 0.20°C/m - 0.40°C/m. Depth shown is depth below lake surface (offshore) or ground level (onshore). Starting temperatures are offset by 20°C for all logs. Temperature profiles project to a surface temperature of about 20°C.

Figure 9. Final temperature profiles for holes exhibiting high thermal gradients, >0.40°C/m. Depth shown is depth below lake surface (offshore) or ground level (onshore). Starting temperatures are offset by 20°C, and profiles project to a surface temperature of about 20°C.

Figure 10. Final temperature profiles for holes exhibiting substantially nonlinear thermal gradients which are not related to changes in lithology (and thus thermal conductivity). Depth shown is depth below lake surface (offshore) or ground level (onshore). Starting temperatures are offset by 20°C for all but the first log, and profiles project to a surface temperature of 20 - 20°C.

Figure 11. Active mud pots located within a few hundred meters of the SSSDP hole (upper right). Craters in foreground are about 1 m in diameter.

Figure 12. Thermal conductivity measured over a 30.5 cm interval of the 1 m core obtained in the bottom of hole RDO6T. Values vary by 40%.

Figure 13. A) Temperature log run in hole RDO6N within a few hours of drilling. B) Thermal conductivity measured on drill cuttings from hole RDO6N by Lee and others (1986, unpublished data). Low temperature zones in the early temperature log, indicative of greater invasion of (cool) drilling fluid is accompanied by increases in thermal conductivity, indicative of greater silt content.

Figure 14. Thermal gradients in the southern Salton Sea region. Contour interval is 0.10°C/m. Lines A-A^1 and B-B^1 indicate the locations of cross-sections shown in Figure 17.

Figure 15. Heat flux in the southern Salton Sea region. Contour interval is 200 mW/m^2. See text for discussion.

Figure 16. Schematic representation of three scales of thermal anomalies at the Salton Sea Geothermal Field. The letter "L" identifies two local features bounded by the

0.5°C/m contour, the Mullet Island Anomaly to the northeast, and the Kornbloom Road anomaly to the southwest, which were discovered during this survey. The Axial Anomaly, modeled by Kasameyer, et al.., 1984, is defined to lie within the 0.3°C/m contour. The approximate boundary of the Broad Anomaly is given by the 0.09°C/m contour, which extends outside the area of thermal measurements. The local anomalies have relatively sharp and well-defined boundaries, but the edge of the broad anomaly is not well defined. Schematic temperature profiles are shown in the inset for the Local (L), Axial (A), and Broad (B) Anomalies, as well as average profiles for the Imperial Valley (V) and the Basin and Range (B+R) average heat flow in sediments.

Figure 17A. Anomalous temperatures in the axial anomaly along line $A-A^1$, shown on Figure 14. The contours represent the anomalous temperatures, in a section along line $A-A^1$ crossing the axial anomaly where its edges are very sharp. The anomalous temperatures were calculated from the actual temperatures by subtracting the idealized temperature profile for the broad anomalous zone, $T(z) = 23°C + 0.10\ z(m)$. Data from wells within two kilometers of the line were projected onto a vertical plane. The vertical black lines indicate portions of wells where temperatures were available. The short vertical lines indicate gradients from shallow wells in Tables I and II, or from Sass et al.., 1984. The temperature profiles from these wells were extrapolated to a depth of 500 m by assuming conductive heat flow. The deep well data is from Younker et al.., 1982. The triangle represents the location of volcanic arc.

Figure 17B. Anomalous temperatures in the axial anomaly along line $B-B^1$, shown on Figure 14. Similar to Figure A except the holes were much closer to the line. Data from State 2-14 (Sass et al., 1987) have been added.

Figure 18. Normal stress in the ground surface for two faults with geometry and

characteristics similar to the Banning-Mission Creek-Brawley fault system (from Full, 1980). Contour interval is $x10^5$ dynes/cm^2. See text for discussion.

Figure 19. Three scales of deformation in the Salton Trough (from Lachenbruch et al., 1985). Dots mark the locations of geothermal fields. Crosshatched areas mark the location of intense modern seismicity (after Fuis et al., 1982). Dashed curves enclose region of basin-wide extension predicted by regional modeling (Lachenbruch et al., 1985). Other features as in Fig. 1.

REFERENCES

Andes, J. P., Jr., M. A. McKibben, Thermal and chemical history of mineralized fractures in cores from the Salton Sea Scientific Drilling Project abst., EOS, 68, 439, 1987.

Atwater, T., Implications of plate tectonics for the Cenozoic tectonic evolution of western North America, Bull. Geol. Soc. Amer., 81, 3513–3536, 1970.

Barelli, A. and A. Palama, A new method for evaluating formation equilibrium temperature in holes during drilling, Geothermics, 10, 95–102, 1981.

Biehler, S., Gravity studies in the Imperial Valley. In: Cooperative Geological–Geophysical Investigations of Geothermal Resources in the Imperial Valley area of California, University of California, Riverside, California, 29–41, 1971.

Blake, M. C., Jr., R. H. Campbell, T. W. Debblee, Jr., D. G. Howell, T. H. Nilsen, W. R. Normark, J. C. Vedder and E. A. Silver, Neogene basin formation in relation to plate-tectonic evolution of the San Andreas Fault System, California, Am. Assoc. Pet. Geol. Bull., 62, 344–372, 1978.

Bredehoeft, J. D. and I. S. Papadopulos, Rates of vertical groundwater movement estimated from the earth's thermal profile, Water Resources Research, 1, 325–328, 1965.

Chinnery, M. A., The deformation of the ground around surface faults, Bull. Seis. Soc. Amer., 51, 355–372, 1961.

Chinnery, M. A., The stress changes that accompany strike-slip faulting, Bull. Seis. Soc. Amer., 53, 921–932, 1963.

Crowell, J. C., Origin of late Cenozoic basins in southern California, in W. R. Dickinson, ed., Tectonics and Sedimentation: Society of Economic Paleontologists and Mineralogists Special Paper, 22, 190–204, 1974.

Elders, W. A. and L. H. Cohen, The Salton Sea geothermal field, California, as a near-field material analog of a radioactive waste repository in salt, Pub. BMI/ONWI-513, 138, Battelle Memorial Inst., Columbus, OH 1983.

Elders, W. A., R. W. Rex, T. Meidav, P. T. Robinson and S. Biehler, Crustal spreading in southern California, Science, 178, no. 4056, 15–24, 1972.

Freund, J. E., Mathematical Statistics, Prentice-Hall, Inc., Englewood Cliffs, NJ, 389p, 1962.

Fuis, G. S., W. D. Mooney, J. H. Healy, G. A. McMechan and W. J. Lutter, Crustal structure of the Imperial Valley region, in the Imperial Valley, California, Earthquake of October 15, 1979, U.S. Geol. Surv. Prof. Pap., 1254, 25–49, 1982.

Fuis, G. S., W. D. Mooney, J. H. Healy, G. A. McMechan and W. J. Lutter, A seismic refraction survey of the Imperial Valley region, California, J. Geophys. Res., 89, 1165–1189, 1984.

Full, W. E., Processes of lithosphere thinning and crustal rifting in the Salton Trough, southern California, Master's Thesis, University of Illinois, 1980.

Goddard, E. N., Chairman, North American Geologic Map Committee, Geologic Map of North America, U.S. Geological Survey, Washington, DC, 1965.

Griscom, A. and L. J. P. Muffler, Aeromagnetic map and interpretation of the Salton Sea geothermal area, California, Geol. Invest. Map, GP 754, U.S. Geol. Surv., Washington, DC, 1971.

Helgeson, H. C., Geologic and thermodynamic characteristics of the Salton Sea geothermal system, Am. J. Sci., 266, 129–166, 1968.

Herzig, C. T. and J. M. Mehegen, ed., Salton Sea scientific drilling project, California State 2-14 well visual core descriptions, UCR/IGPP-86/1, 1986.

Hill, D. P., P. Mowinckel and Z. G. Peake, Earthquakes, active faults and geothermal areas in the Imperial Valley, California, Science, 188, 1306–1308, 1975.

Jaeger, J. C., Application of the theory of heat conduction to geothermal measurements, in Terrestrial Heat Flow, W. H. K. Lee, ed., AGU Mangr., 8, 7–23, 1965.

Kasameyer, P. W., L. W. Younker and J. M. Hansen, Development and application of a hydrothermal model for the Salton Sea geothermal field, California, Geol. Soc. Am. Bull., 95, 1242-1252, 1984.

Kasameyer, P. W. and J. R. Hearst, Borehole gravity measurements in the Salton Sea scientific drilling program, Well State 2-14, submitted to J. Geophys. Res., 1987.

Kelley, V. C. and J. L. Saske, Origin of the Salton volcanic domes, Salton Sea, California, Jour. Geol., 44, 496-509, 1936.

Lachenbruch, A. H., Thermal effects of the ocean on permafrost, Bull. Geol. Soc. Amer., 68, 1515-1530, 1957.

Lachenbruch, A. H., J. H. Sass and S. P. Galanis, Jr., Heat flow in southernmost California and the origin of the Salton Trough, J. Geophys. Res., 90, 6709-6736, 1985.

Lee, T-C and L. Cohen, Onshore and offshore measurements of temperature gradients in the Salton Sea geothermal area, California, Geophysics, 44, 206-215, 1979.

Lee, T-C, T. L. Henyey and B. N. Daniata, A simple method for the absolute measurement of thermal conductivity of drill cuttings, Geophysics, 51, 1580-1584, 1986.

Lilje, A. and J. M. Mehegan, ed., Salton Sea scientific drilling project, California state 2-14 well core summaries, UCR/IGPP-86/2, 1986.

Lomnitz, C., F. Mooser, C. R. Allen, J. N. Brune and W. Thatcher, Seismicity and tectonics of the northern Gulf of California region, Mexico: Preliminary results, Geofis. Int., 10, 37-48, 1970.

Muramoto, F. S., W. A. Elders, Correlation of wireline log characteristics with hydrothermal alteration and other reservoir properties of the Salton Sea and Westmorland Geothermal Fields, Imperial Valley, California, USA, Los Alamos National Laboratory Report LA-10128-MS, Los Alamos, New Mexico, 1984.

Newmark, R. L., P. W. Kasameyer, L. W. Younker and P. C. Lysne, Research drilling at the Salton Sea geothermal field, California: The shallow thermal gradient project, EOS, 67, 698-707, 1986.

Rex, R. W., The origin of brines of the Imperial Valley, California, Geotherm. Res. Counc. Trans., 7, 321, 1983.

Riney, T. D., J. W. Pritchett, and S. K. Garg, Salton Sea geothermal reservoir simulation, paper presented at the Third Workshop on Reservoir Engineering, Stanford University, 1977.

Robinson, P. T., W. A. Elders and L. J. P. Muffler, Quaternary volcanism in the Salton Sea Geothermal Field, Imperial Valley, California, Geol. Soc. A. Bull., 87, 347–360, 1976.

Rodgers, D. A., Analysis of basin development produced by en echelon strike slip faults, in P. F. Ballance and H. C. Reading, eds., Oxford, England, International Association of Sedimentologists, 27–41, 1980.

Sass, J. H., S. P. Galanis, Jr., A. H. Lachenbruch, B. V. Marshall and R. J. Munroe, Temperature, thermal conductivity, heat flow, and radiogenic heat production from unconsolidated sediments of the Imperial Valley, California, U.S. Geol. Surv. Open File Rep., 84–490, 37pp, 1984.

Sass, J. H., S. S. Priest, L. E. Duda, C. C. Carson, J. D. Hendricks and L. C. Robinson, Thermal regime of the State 2–14 well, Salton Sea scientific drilling project, submitted to J. Geophys. Res., 1987.

Sturtevant, R. G. and A. E. Williams, Oxygen isotopic profiles for the State 2–14 Geothermal Well: Evidence for a complex thermal history, abst., EOS, 68, 445, 1987.

Von Herzen, R. P. and A. E. Maxwell, The measurement of thermal conductivity of deep sea sediments by a needle probe method, J. Geophys. Res., 64, 1557–1563, 1959.

Von Herzen, R. P. and S. Uyeda, Heat flow through the eastern Pacific ocean floor, J. Geophys. Res., 68, no. 14, 4219–4250, 1963.

Younker, L. W., P. W. Kasameyer and J. Tewhey, Geological, geophysical and thermal characteristics of the Salton Sea geothermal field, California, J. Volcanol. Geotherm. Res., 12, 221, 1982.

*Disclaimer: This document was prepared as an account of work sponsored by an agency of the United States Government. Neither the United States Government nor the University of California, nor any of their employees, makes any warranty, express or implied, or assumes any legal liability or responsibility for the accuracy, completeness, or usefulness of any information, apparatus, product, or process disclosed, or represents that its use would not infringe privately owned rights. Reference herein to any specific commercial products, process, or service by trade name, trademark, manufacturer, or otherwise, does not necessarily constitute or imply its endorsement, recommendation, or favoring by the United States Government or the University of California. The views and opinions of authors expressed herein do not necessarily state or reflect those of the United States Government or the University of California, and shall not be used for advertising or product endorsement purposes.

Table I. Kennecott/Bear Creek Mining Program

Hole #	Location		Date Drilled	Last Temperature Log	Thermal Gradient		Heat Flow
	Latitude ^{o}N	Longitude ^{o}W			($^{o}C/m$)	95% Conf.[2] ($^{o}C/m$)	(mW/m^2)
P1-1	33.184	115.675	08/23/82	10/20/82	.1143	.0034	177
P1-2	33.169	115.692	08/31/82	09/25/82	.1390	.0021	252
P1-4	33.155	115.708	08/28/82	10/20/82	.1096	.0021	209
P1-5	33.148	115.692	08/29/82	10/20/82	.1785	.0031	322
P1-6	33.155	115.675	08/30/82	10/20/82	.5001	.0111	996
P1-7	33.141	115.726	08/26/82	10/20/82	.0837	.0037	137
P1-8	33.133	115.708	08/27/82	10/20/82	.0839	.0019	151
P1-9	33.133	115.683	08/30/82	10/20/82	.1172	.0035	212
P1-11	33.118	115.726	08/25/82	10/15/82	.0699	.0030	108
P1-14	33.125	115.667	07/21/82	10/11/82	.1815	.0038	204
P1-17	33.104	115.708	08/24/82	10/15/82	.0710	.0031	129
P1-19	33.104	115.683	05/18/82	07/14/82	.0734	.0018	94
P1-20	33.104	115.672	05/17/82	07/02/82	.0582	.0017	92
P2-1	33.321	115.623	07/16/82	10/11/82	.0857	.0019	111
P2-2	33.307	115.614	07/10/82	10/11/82	.1016	.0016	100
P2-4	33.293	115.606	07/08/82	10/11/82	.1017	.0022	100
P2-6	33.278	115.597	07/07/82	10/11/82	(NL)[1]	****	***
P2-9	33.264	115.588	07/19/82	10/11/82	(NL)[1]	****	***
P2-10	33.250	115.588	07/05/82	10/11/82	(NL)[1]	****	***
P2-11A	33.250	115.579	07/03/82	10/11/82	.1780	.0123	338
P2-13	33.235	115.579	05/13/82	05/20/82	(NL)[1]	****	***
P2-14	33.227	115.579	05/11/82	07/02/82	.1894	.0086	299
P2-15	33.220	115.570	07/02/82	10/11/82	.1996	.0068	255

Hole #	Location		Date Drilled	Last Temperature Log	Thermal Gradient		Heat Flow
	Latitude °N	Longitude °W			(°C/m)	95% Conf.[2] (°C/m)	(mW/m^2)
P3-2	33.307	115.649	08/10/82	09/24/82	.0730	.0045	105
P3-3	33.307	115.632	08/08/82	10/17/82	.0870	.0029	94
P3-7	33.293	115.632	08/13/82	10/17/82	.0853	.0041	125
P3-9	33.286	115.623	08/14/82	10/17/82	.0890	.0025	109
P3-10	33.278	115.632	08/15/82	09/24/82	.1032	.0039	175
P3-12	33.271	115.623	08/16/82	10/17/82	.0965	.0043	136
P3-15	33.264	115.606	08/17/82	10/17/82	.1060	.0038	219
P3-17	33.250	115.606	08/18/82	10/17/82	.2217	.0128	380
P3-20	33.235	115.587	08/22/82	10/17/82	.4469	.0155	793
P4-9	33.141	115.667	07/20/82	08/20/82	.7434	.0169	1421
P4-13	33.118	115.692	07/30/82	10/12/82	.1074	.0025	217
P4-14	33.090	115.731	07/30/82	10/12/82	.0556	.0015	97
P4-16	33.090	115.692	07/23/82	10/12/82	.0666	.0026	77
P4-17	33.082	115.717	07/28/82	10/12/82	.0800	.0023	80
P4-18	33.082	115.701	07/26/82	10/12/82	.0744	.0038	101
P6-4	33.082	115.701	9/9-12/82	10/16/82	.0801	.0018	83

[1] (NL) = nonlinear temperature profile where changes in thermal gradient are apparently not related to changes in dominant lithology.

[2] Using the relationship described by Freund (1962).

Table II. Shallow Salton Thermal Gradient Project (LLNL/SNL)

Hole #	Location		Date Drilled	Last Temperature Log	Thermal Gradient		Heat Flow
	Latitude °N	Longitude °W			(°C/m)	95% Conf.[3] (°C/m)	(mW/m^2)
RD06D[1]	33.249	115.658	11/24/85	--------	----	----	---
RD06E	33.264	115.640	12/10/85	01/08/86	.1542	.0006	284
RD06K	33.169	115.649	12/01/85	04/04/86	.3129	.0010	503
RD06N	33.242	115.606	12/08/85	04/05/86	.5068	.0024	866
RD06T	33.235	115.632	11/23/85	04/05/86	.2691	.0012	516
RD06U	33.227	115.614	12/09/85	04/03/86	.4439	.0133	1212
RD06Y	33.220	115.623	11/19/85	01/10/86	.2142	.0072	383
RD06Z	33.206	115.623	11/25/85	04/05/86	.1953	.0007	353
RD07A	33.220	115.606	11/17/85	04/03/86	(NL)[2]	****	***
RD07B	33.213	115.597	11/16/85	04/04/86	.7966	.0015	1317
RD07E	33.198	115.649	11/16/85	02/05/86	.0883	.0007	161
RD07F	33.184	115.640	11/27/85	02/05/86	.1097	.0007	204
RD07I	33.191	115.623	12/26/85	04/04/86	.2689	.0008	498
RD07M	33.162	115.683	12/06/85	02/05/86	.2126	.0007	383
RD07P	33.169	115.667	12/07/85	02/05/86	.0902	.0006	175
RD07S	33.148	115.667	12/05/85	02/05/86	.8331	.0021	1488
RD07U	33.133	115.667	12/04/85	04/04/86	.3113	.0011	644
RD07Y	33.162	115.658	12/02/85	04/04/86	.1394	.0009	265
RD072	33.155	115.662	12/13/85	04/04/86	.3535	.0009	556

1 Hole RD06D was lost before any temperature logs were obtained.

2 (NL) = nonlinear temperature profile where changes in thermal gradient are apparently not related to changes in dominant lithology.

3 Using the relationship described by Freund (1962).

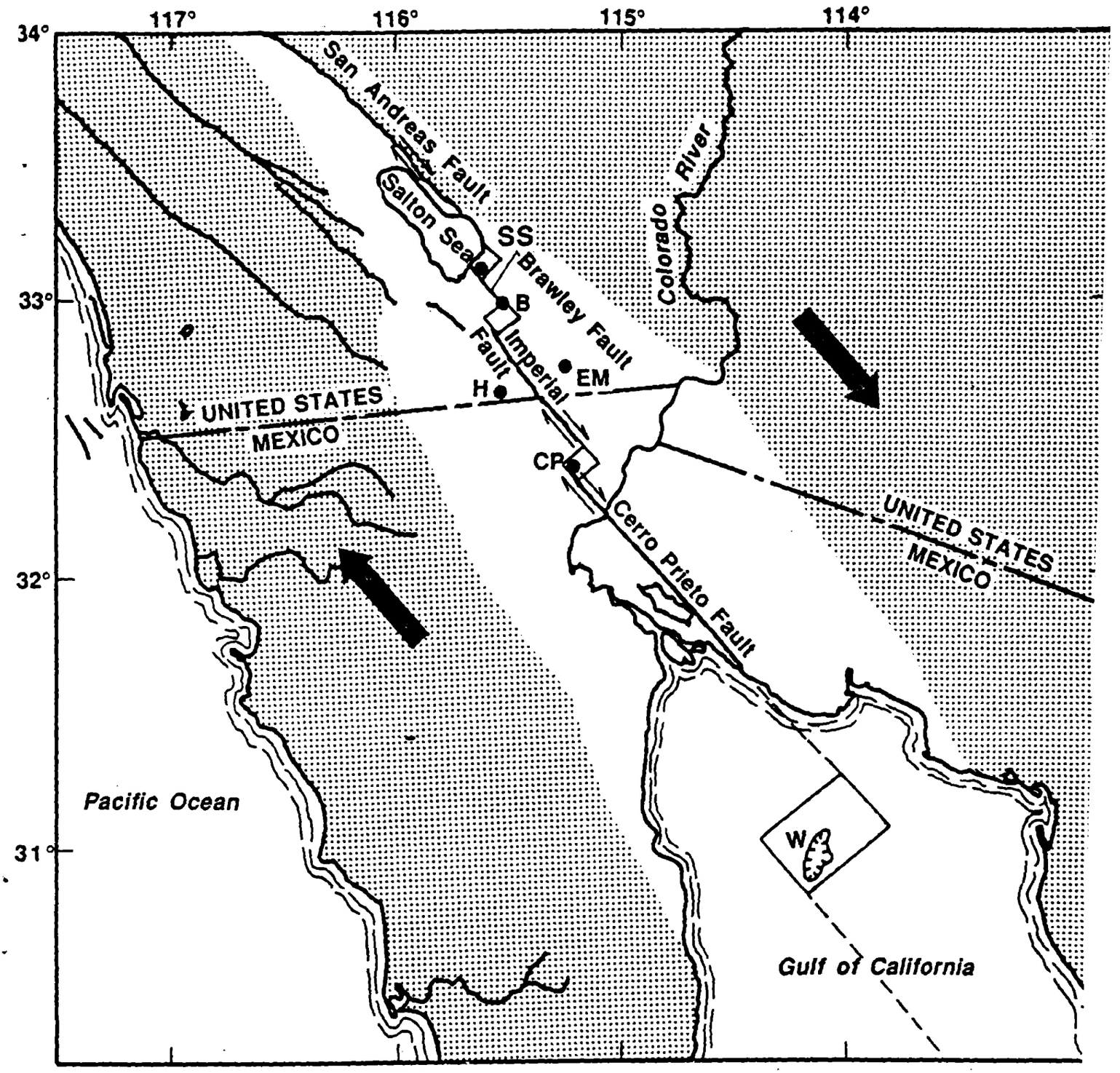

Figure 1 Newmark

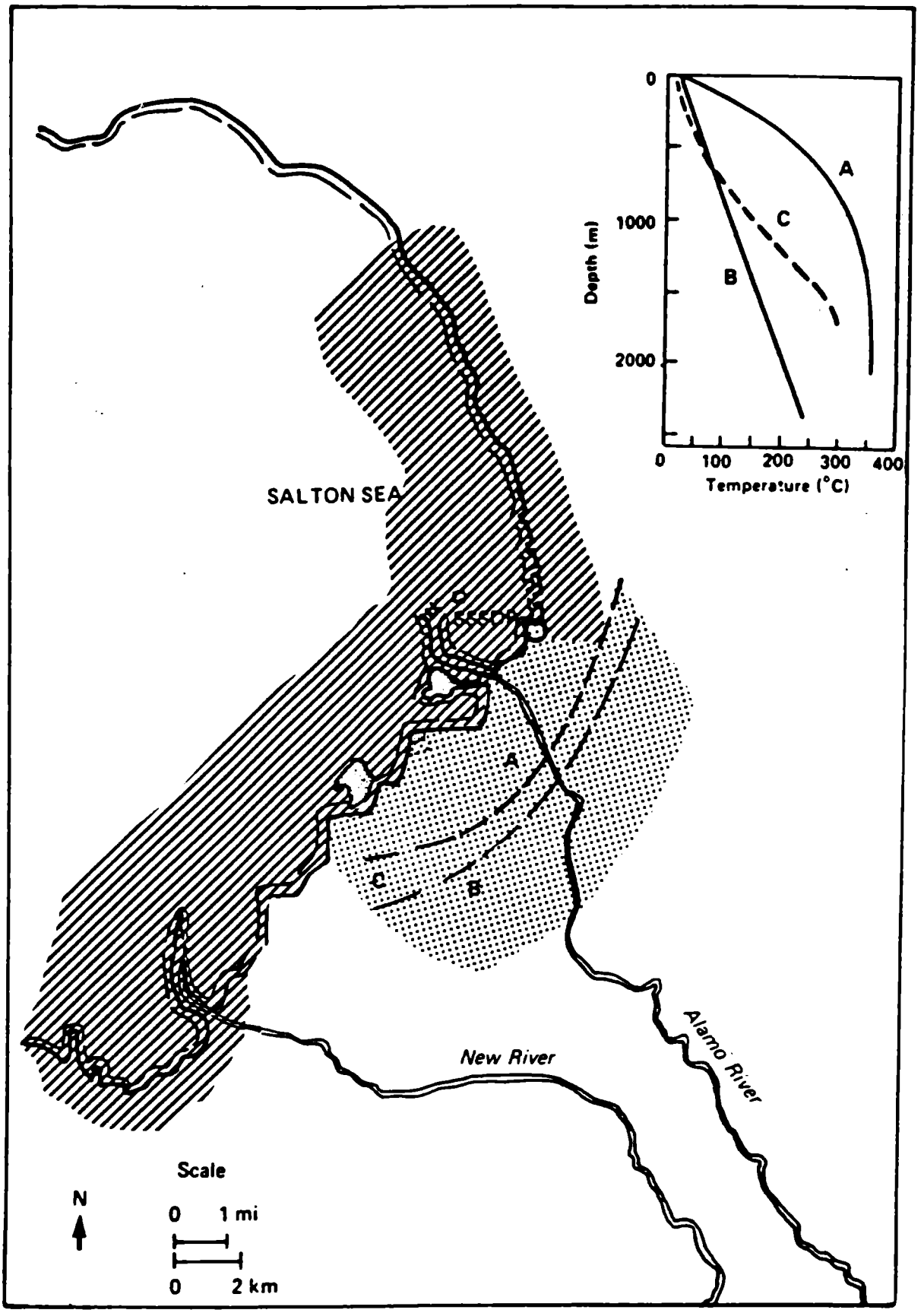

Figure 2 Newmark

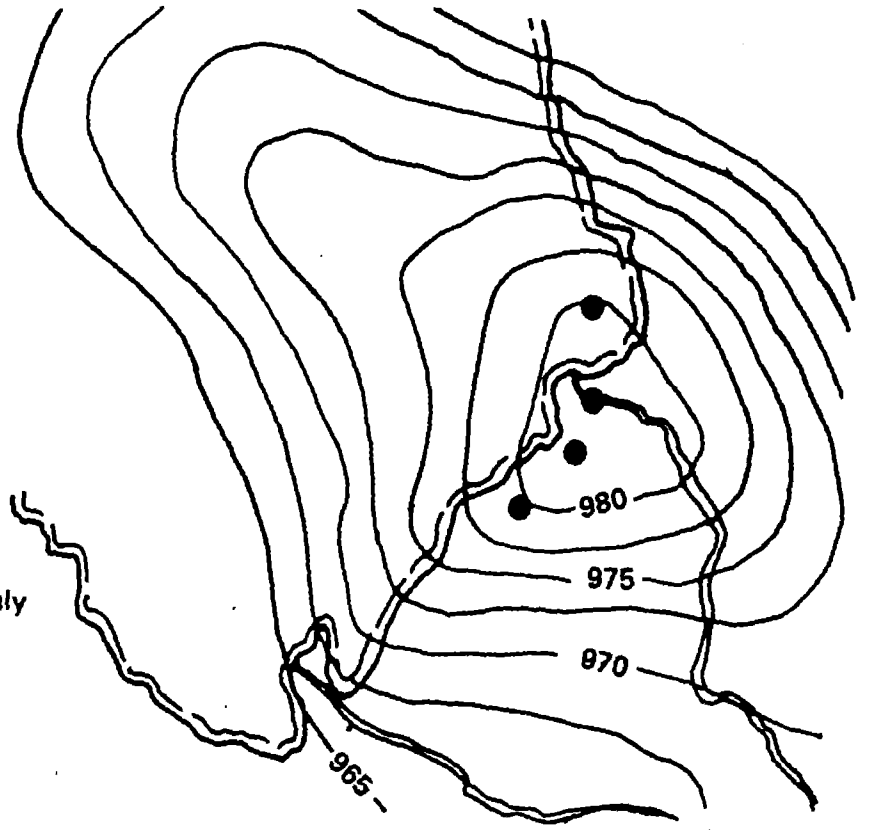

A)

Salton Sea Gravity
Complete Bouguer Anomaly
(after Biehler, 1971)

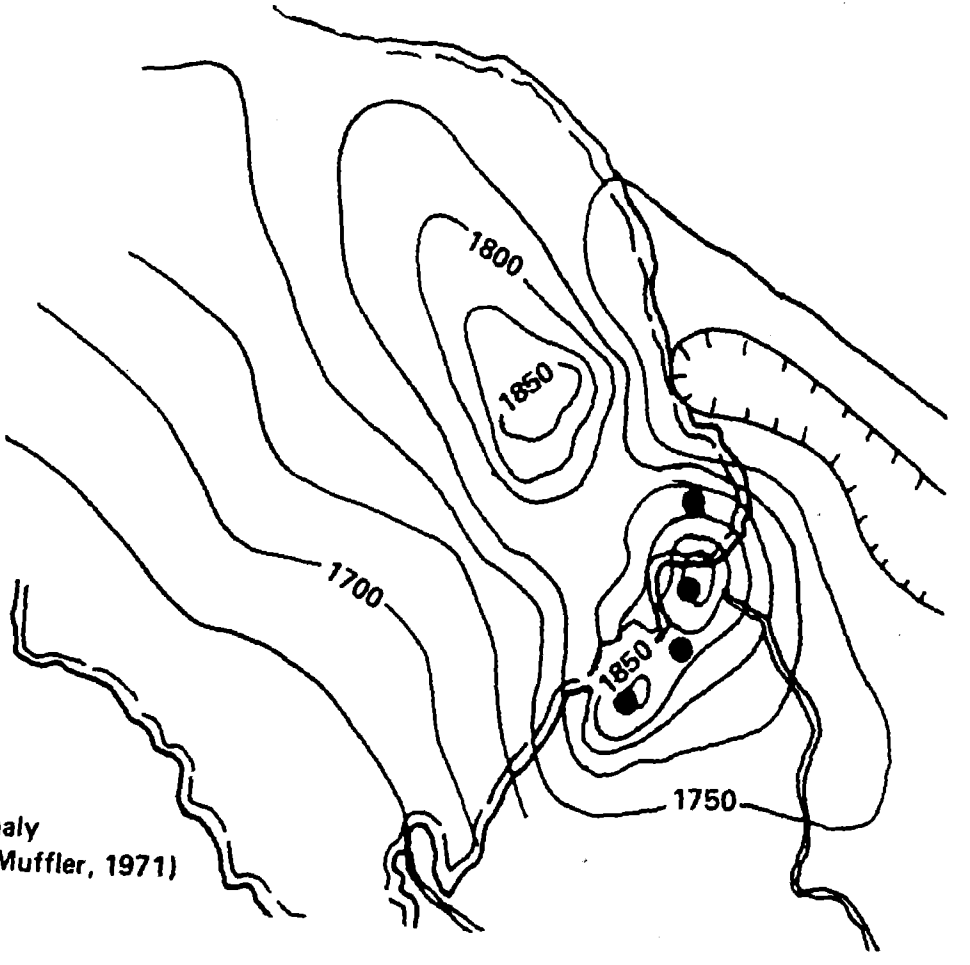

B)

Aeromagnetic Anomaly
(After Griscom and Muffler, 1971)

Figure 3 Newmark

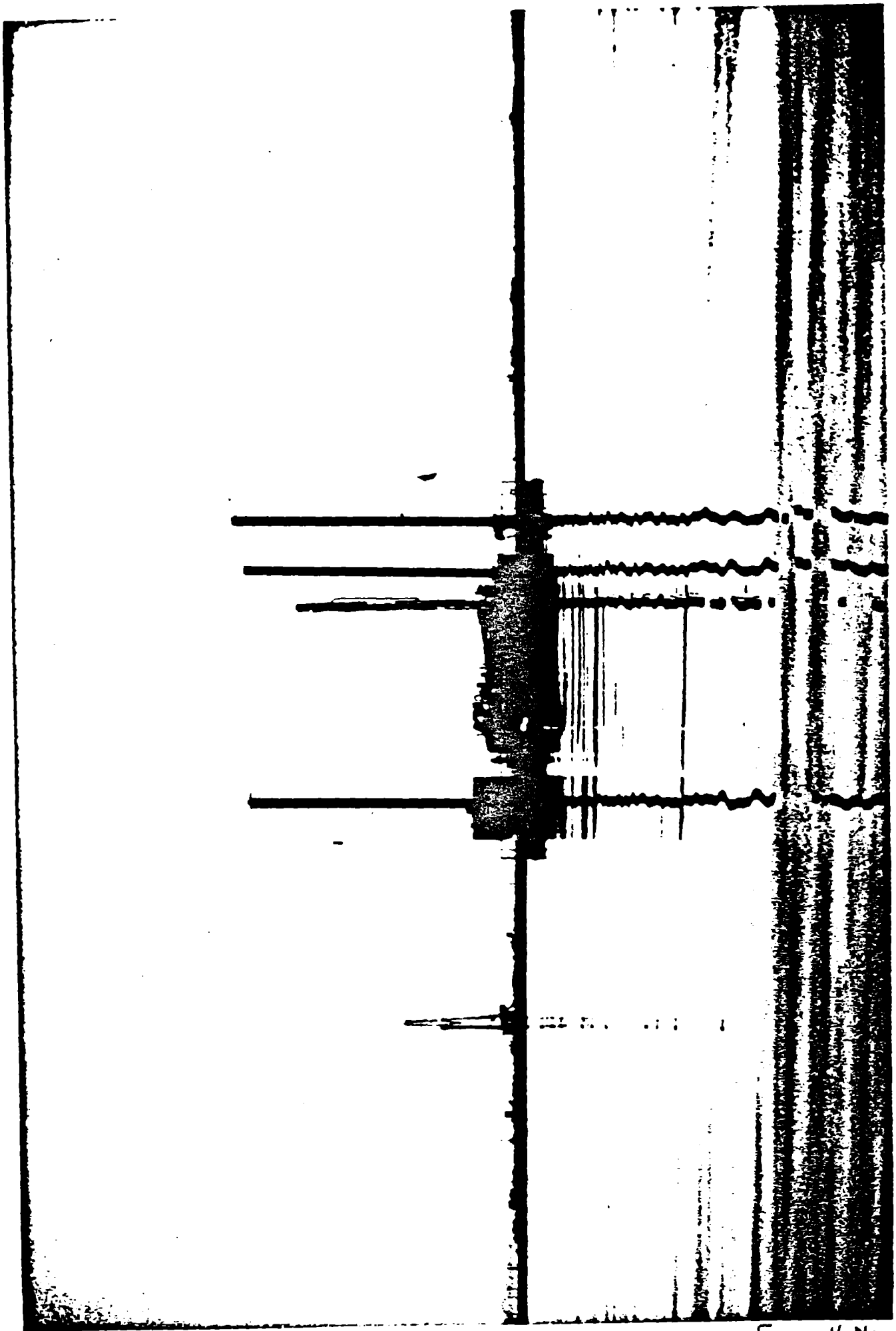

Figure 4 Newmark

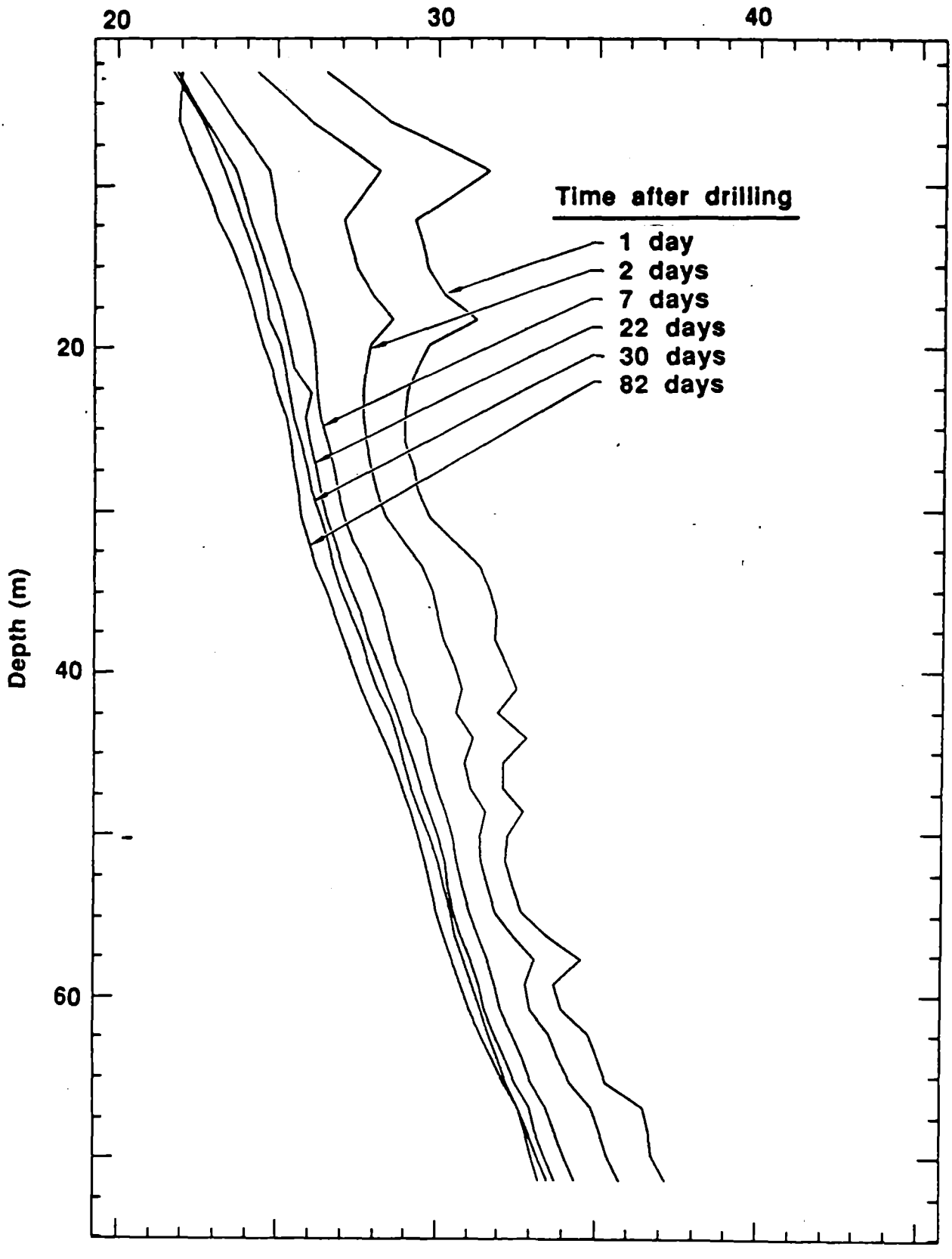

Figure 5 Newmark

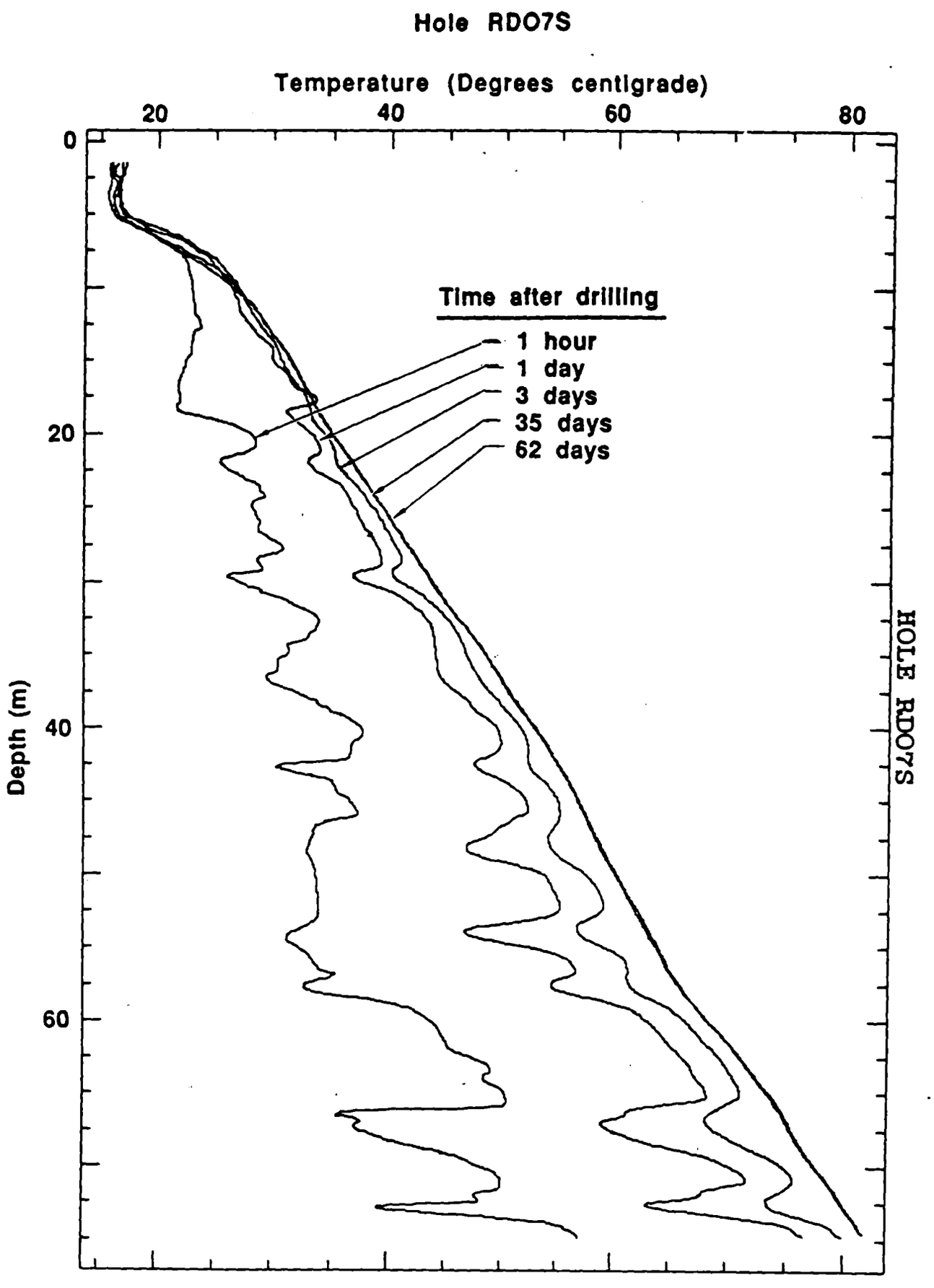

Figure 6 Newman

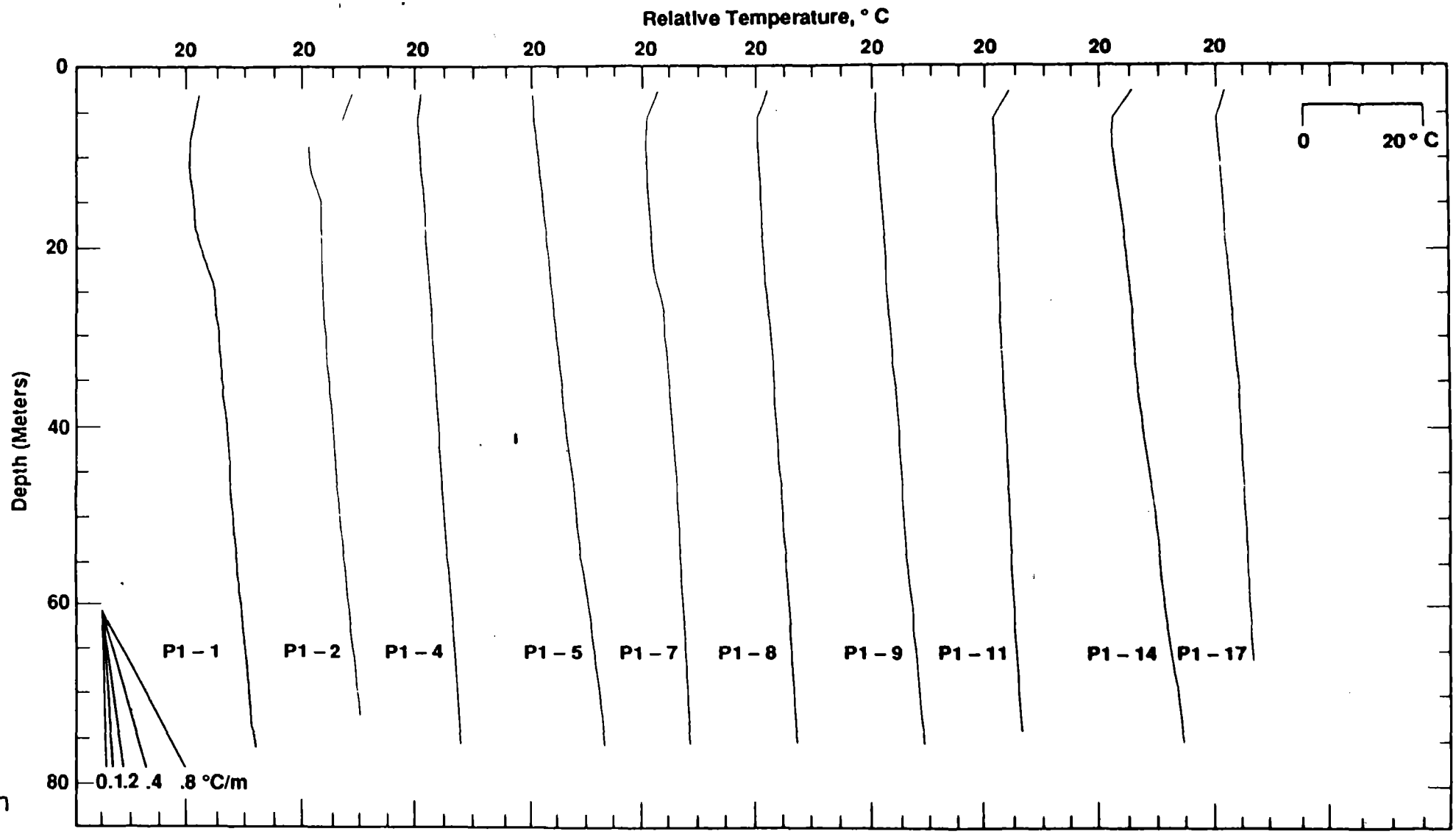

Figure 7A Newmark

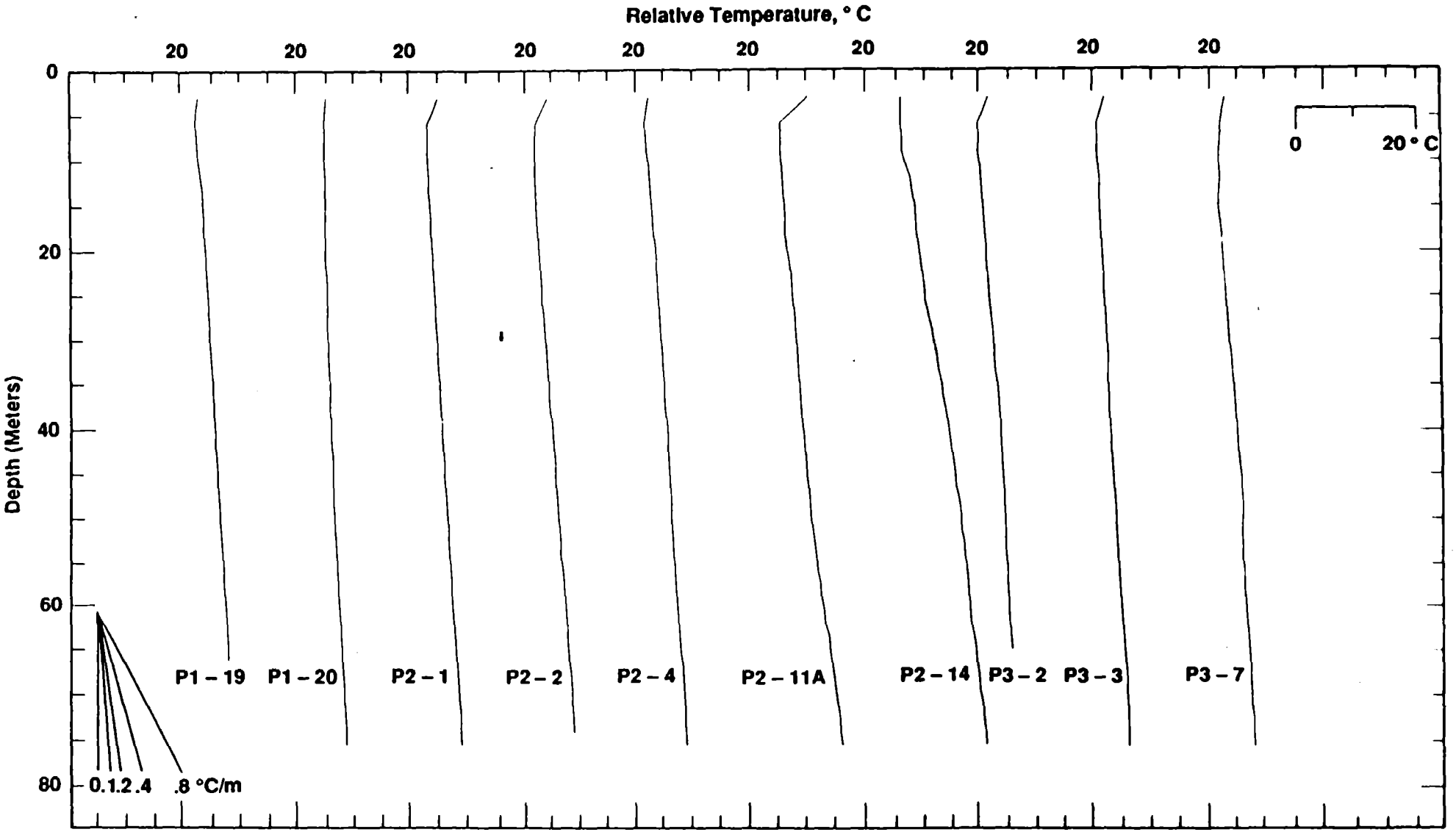

Figure 16 Newark

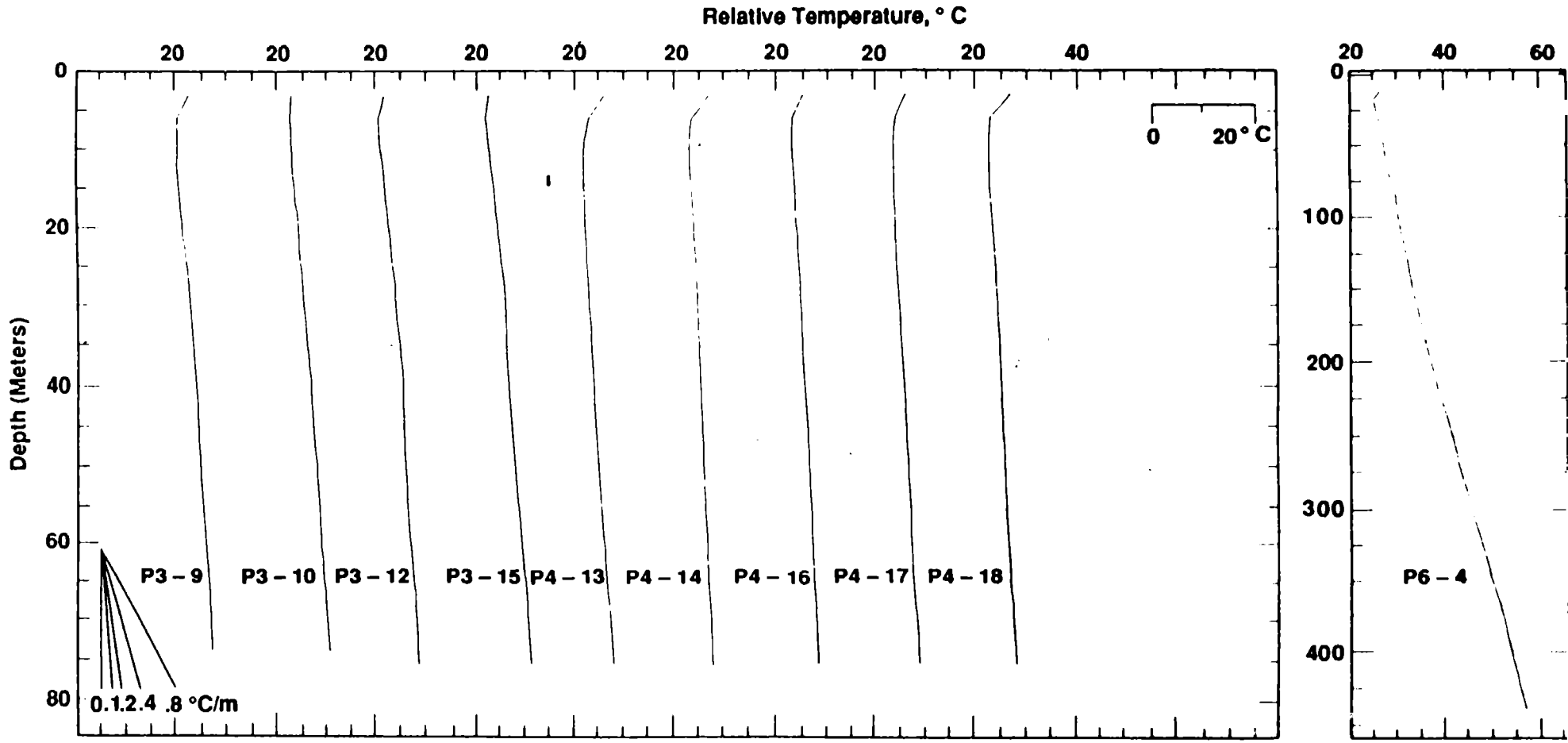

Figure 7C Newmark

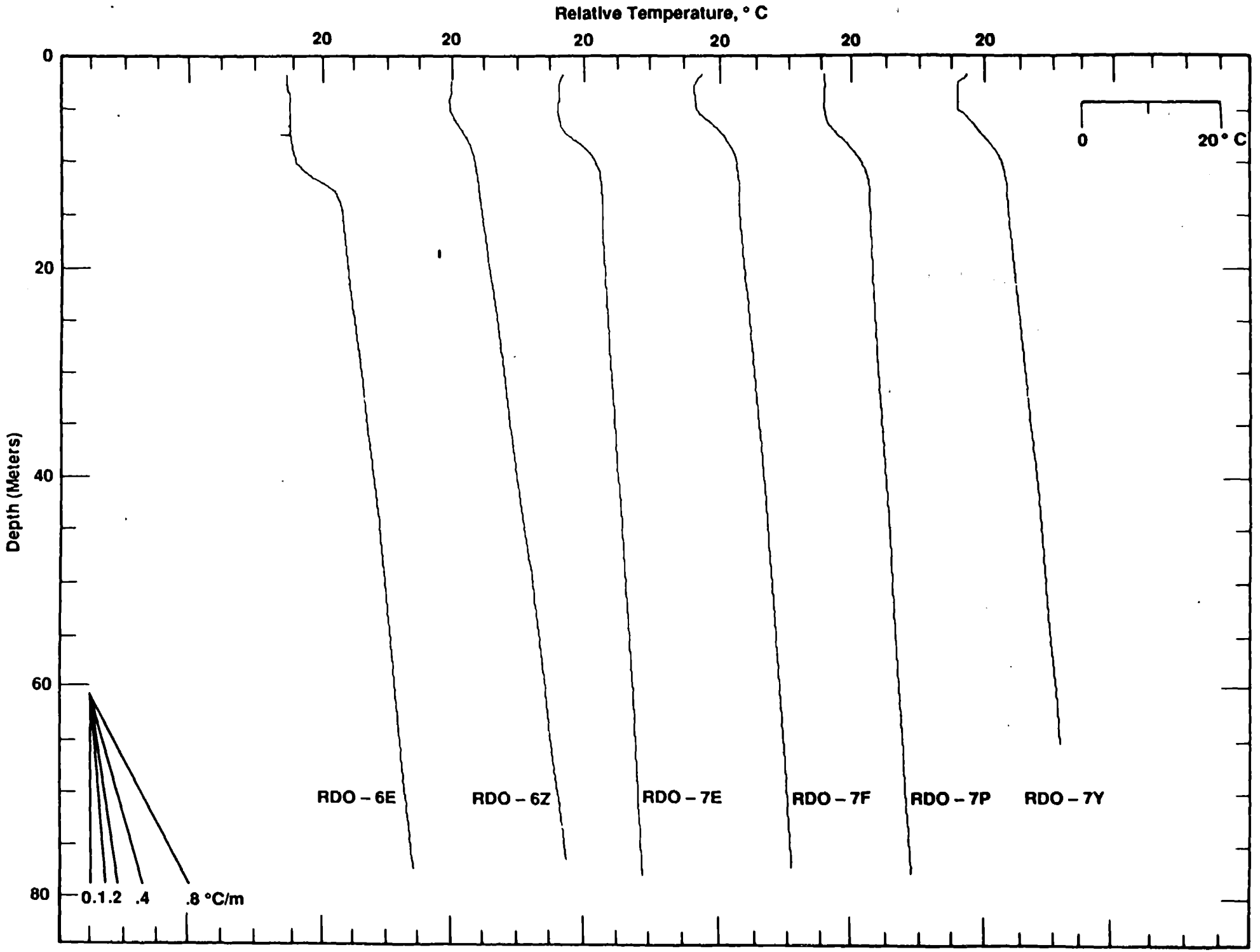

Figure 7d Newman

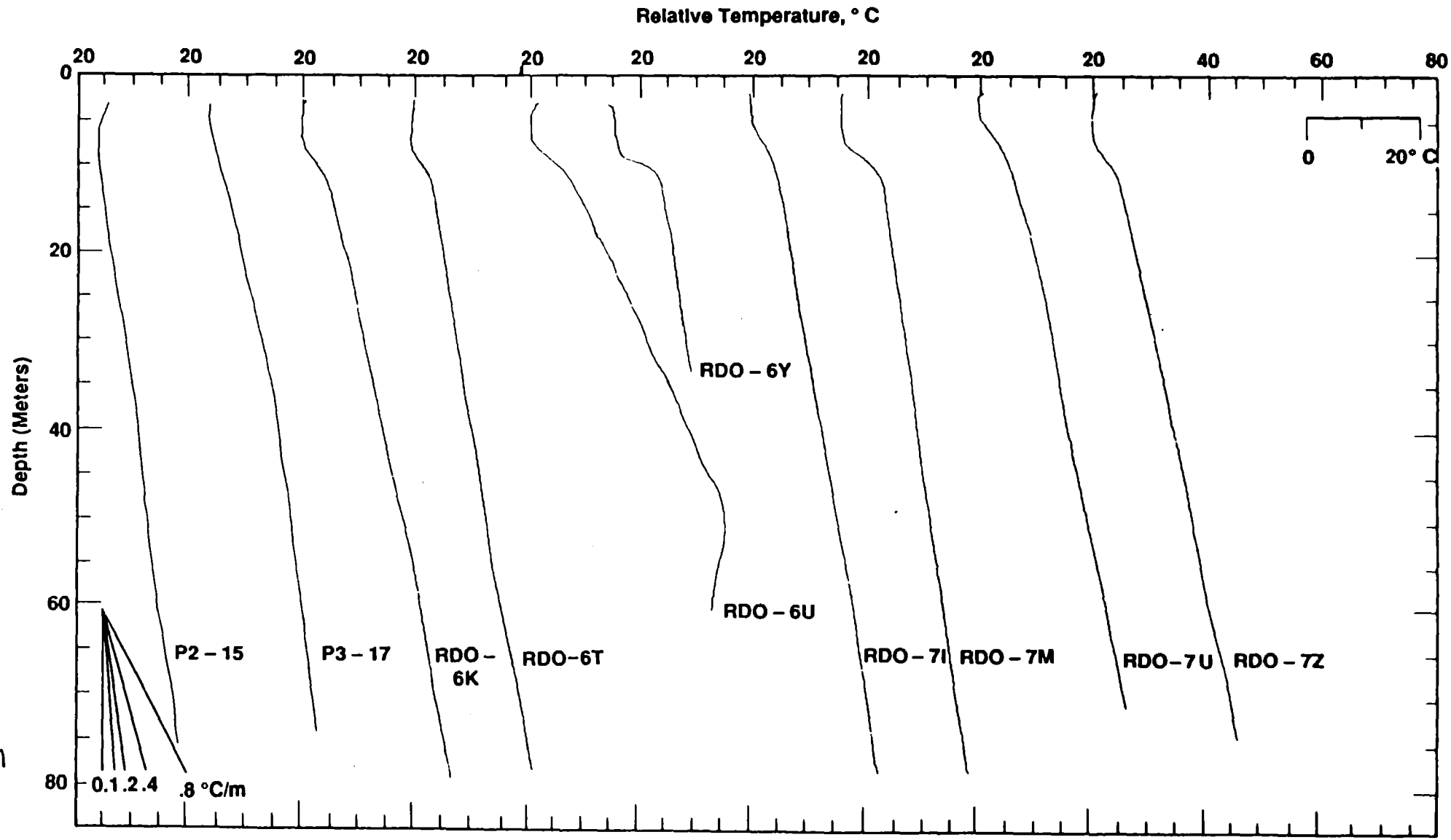

Figure 8 Newman

Figure 9 Newmark

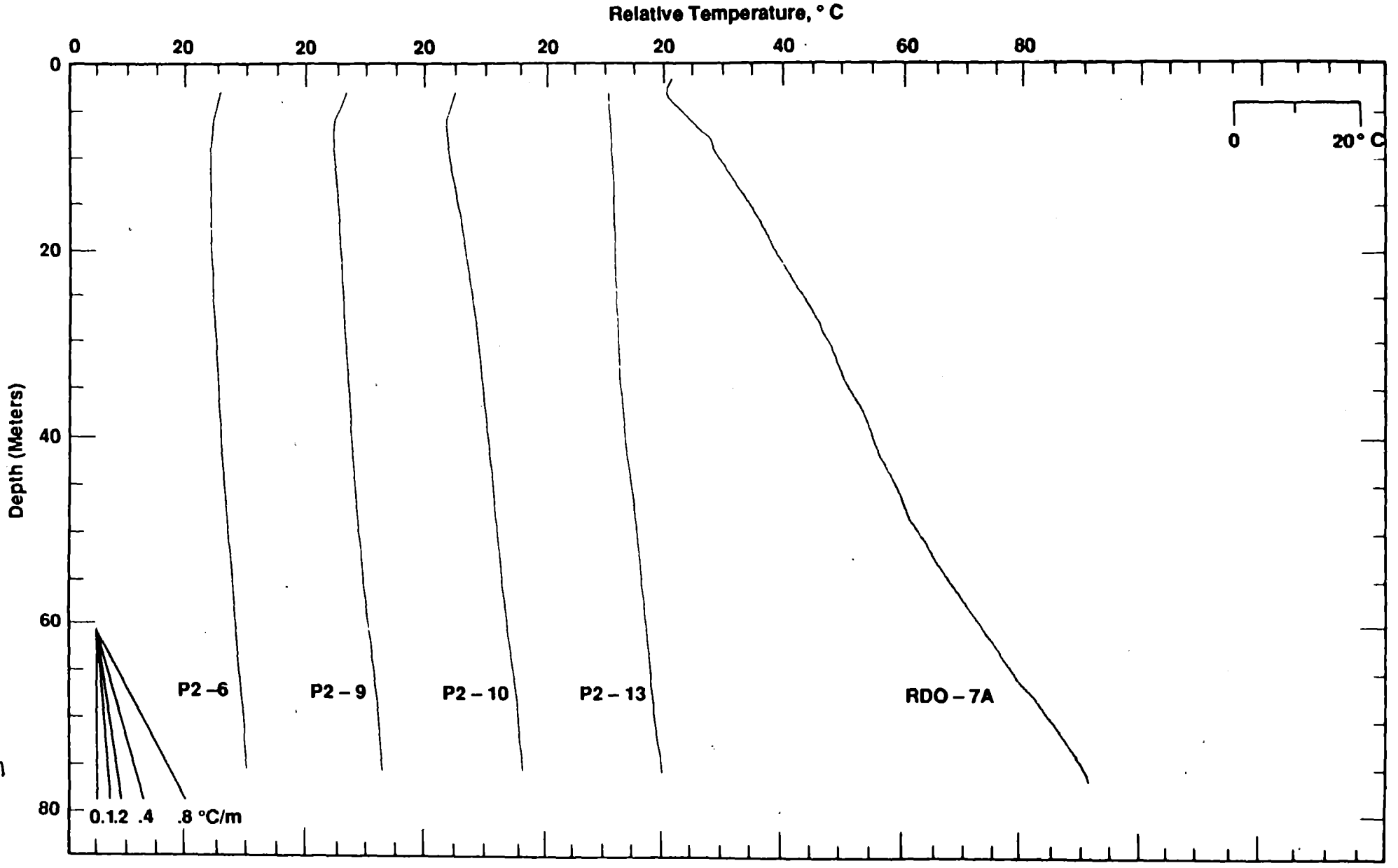

Figure 10 Nkumer

Figure 11 Newmark

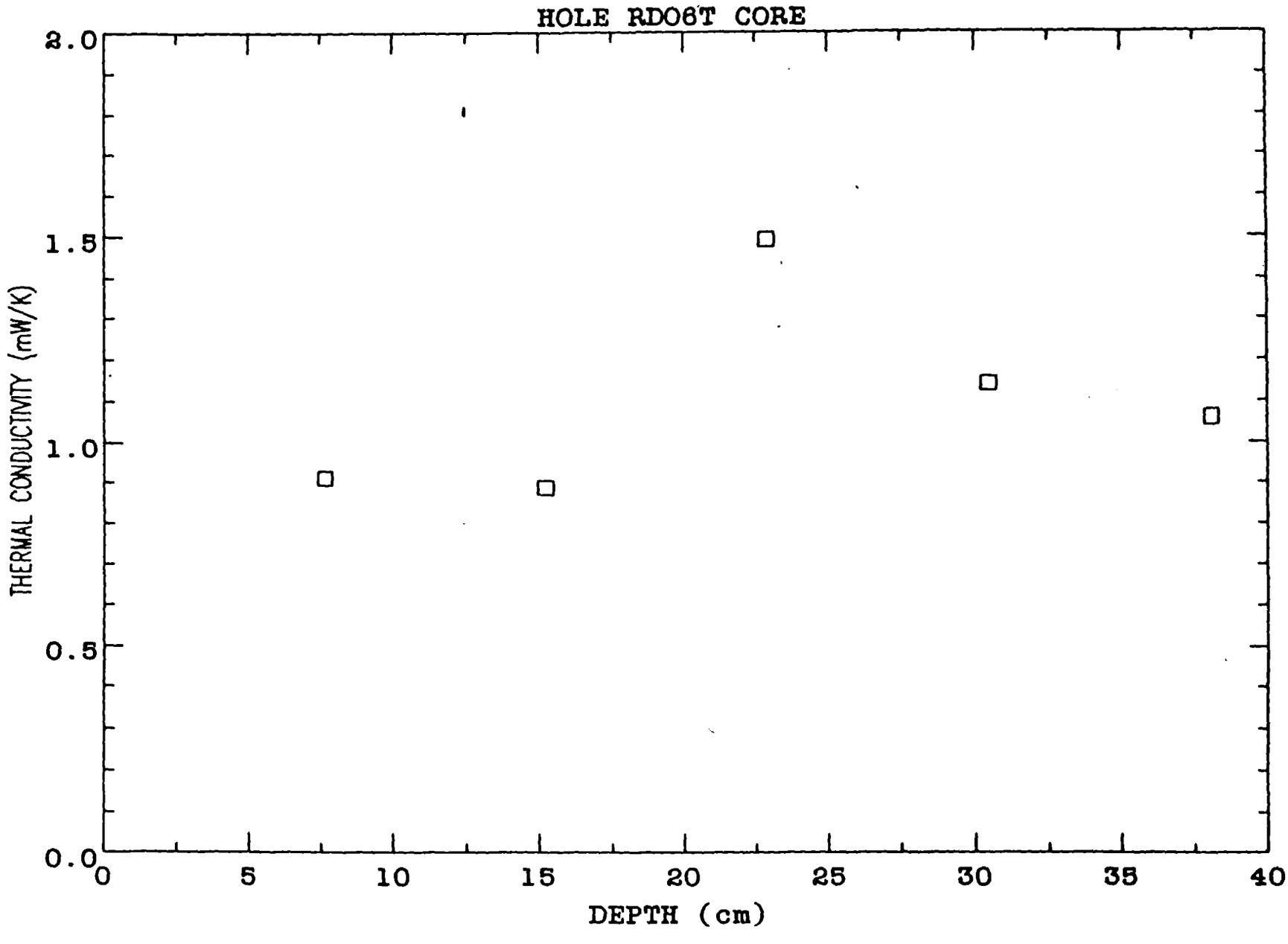

Figure 12 Newmark

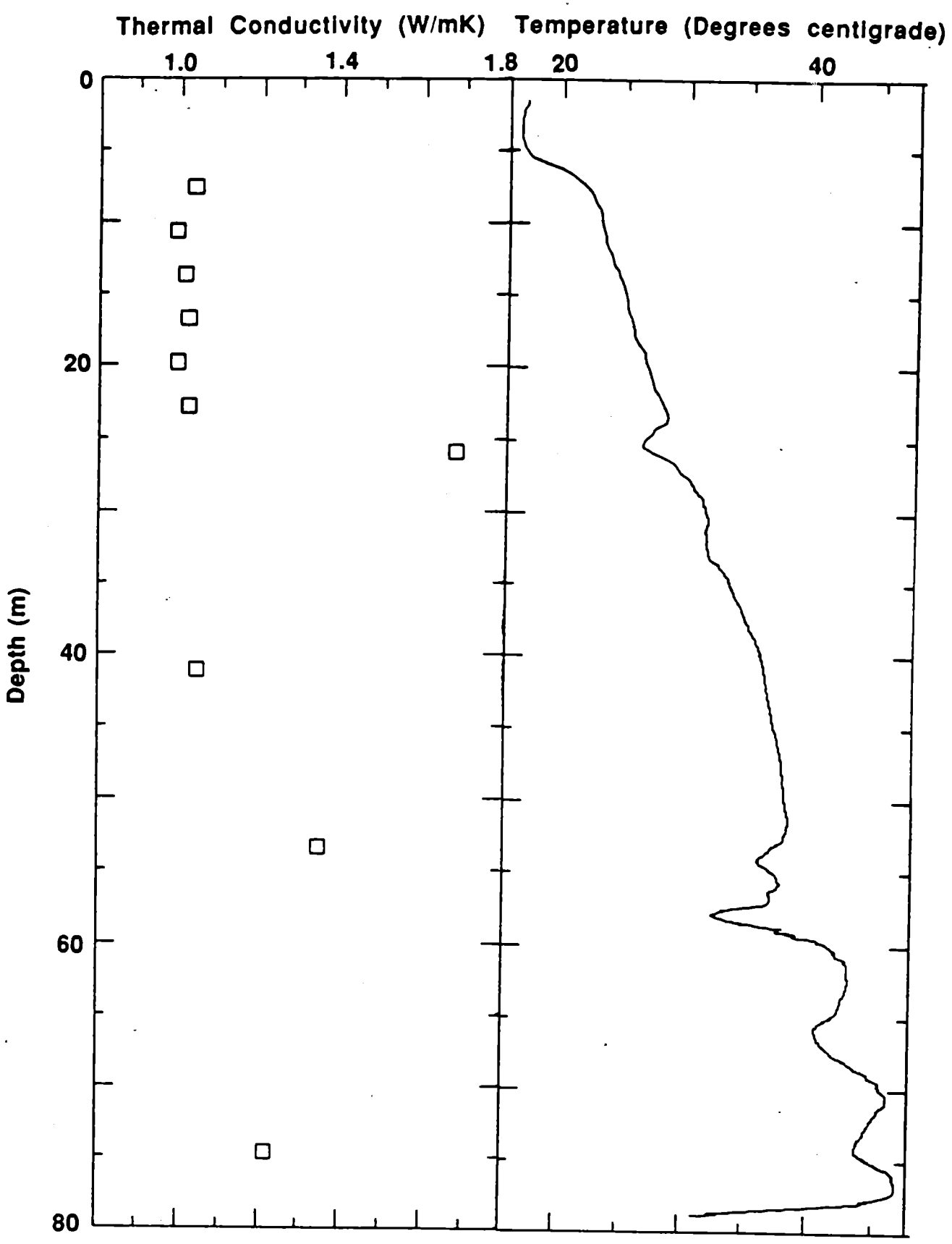

Figure 13 Newmark

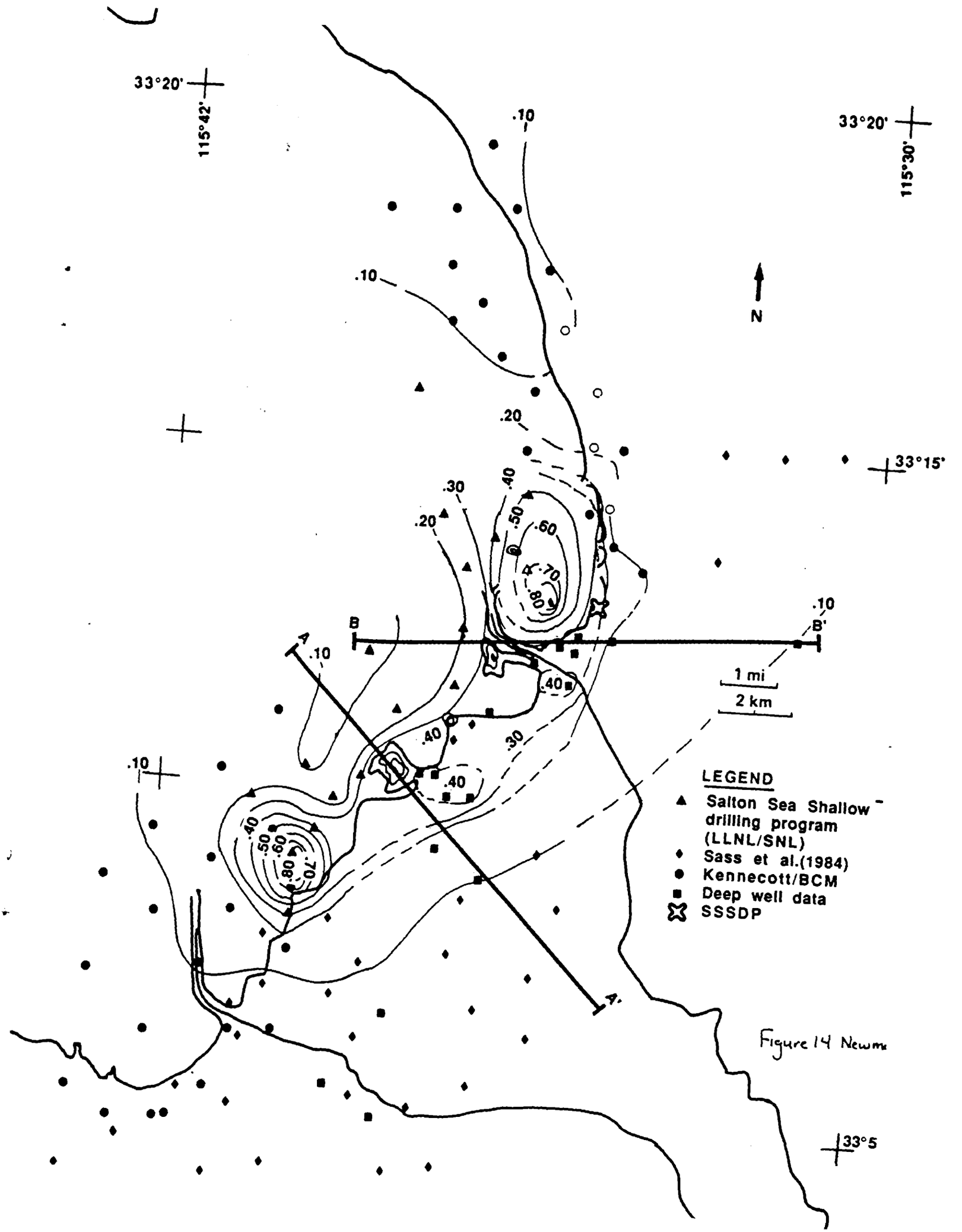

Figure 14 Newm

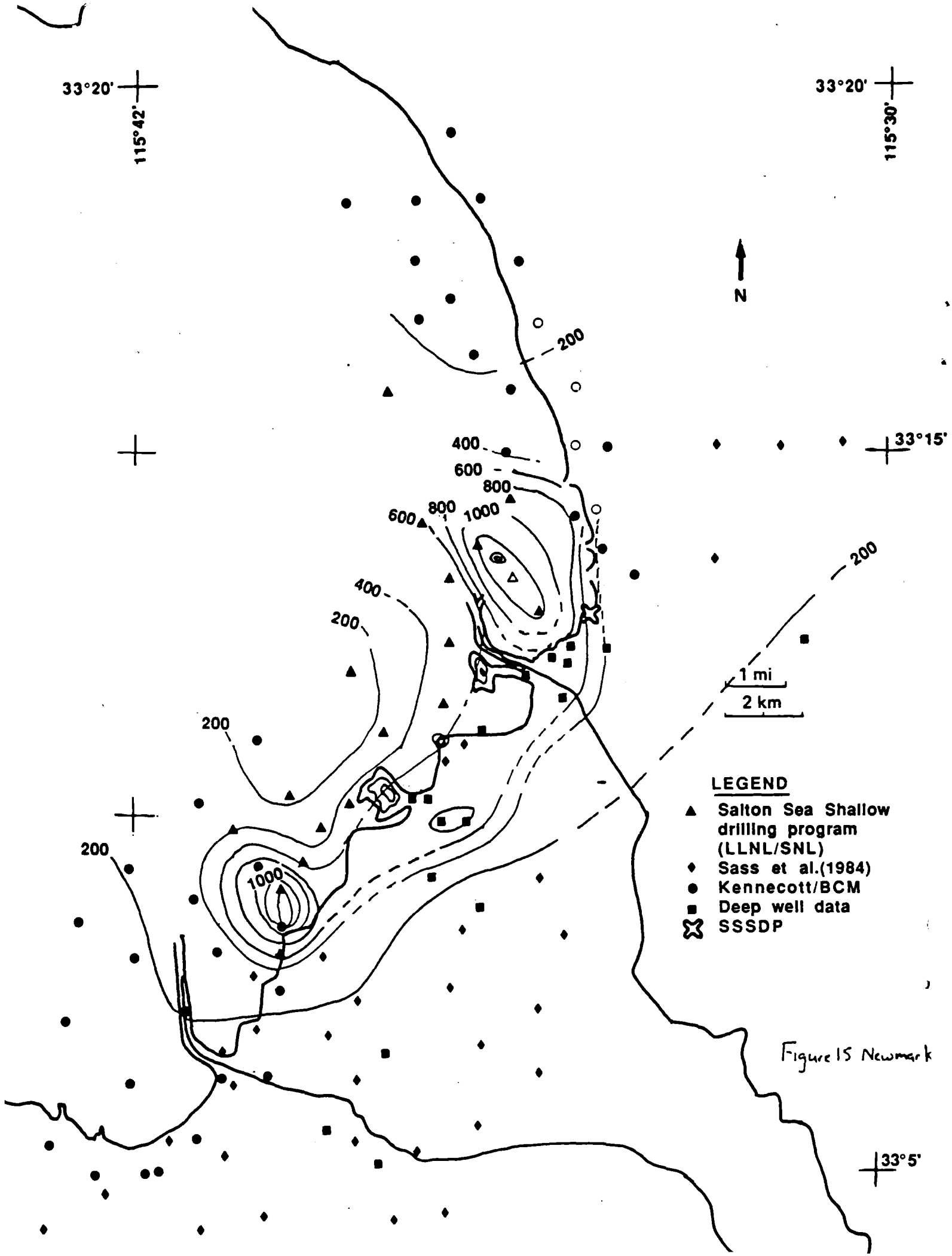

Figure 15 Newmark

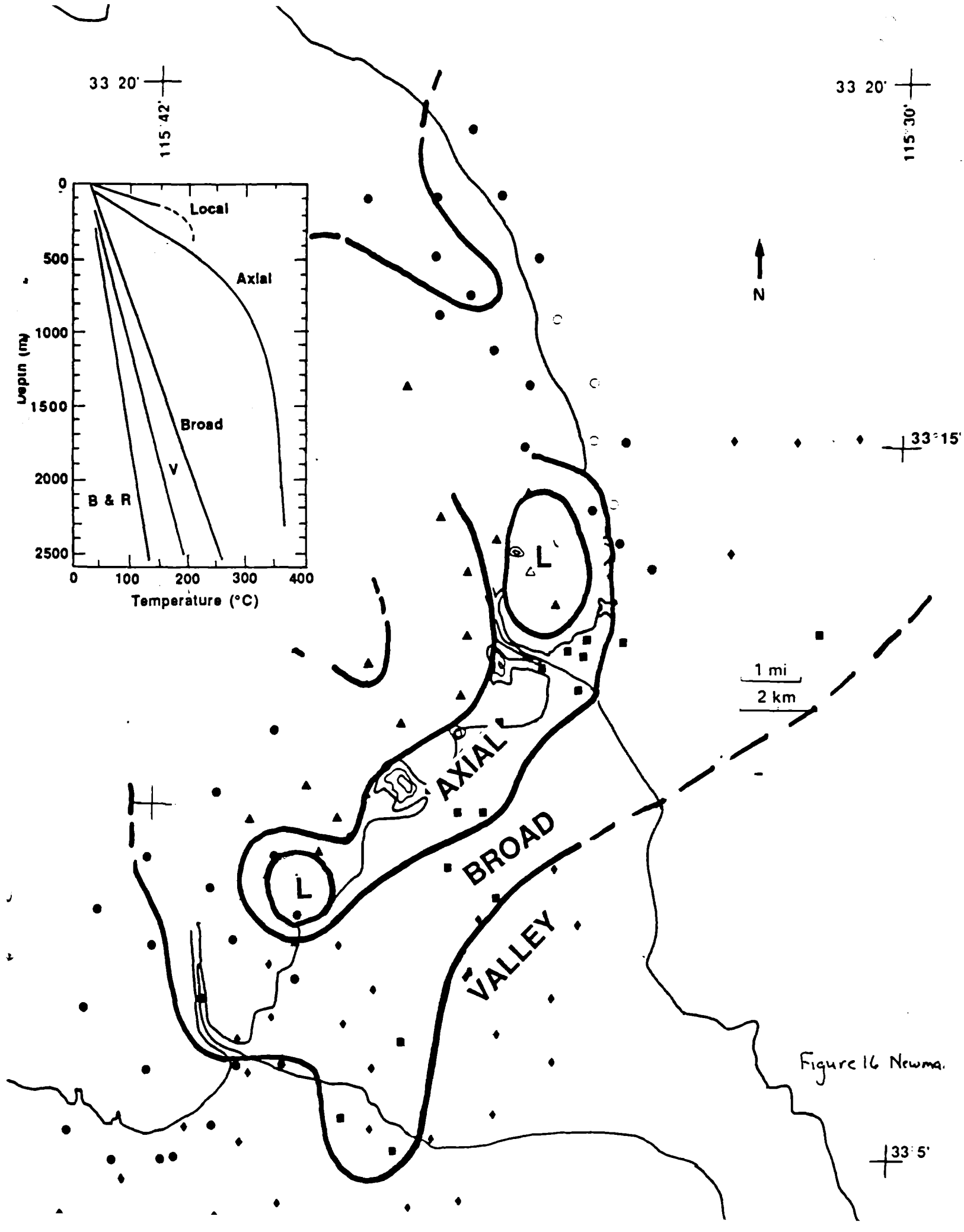

Figure 16 Newma

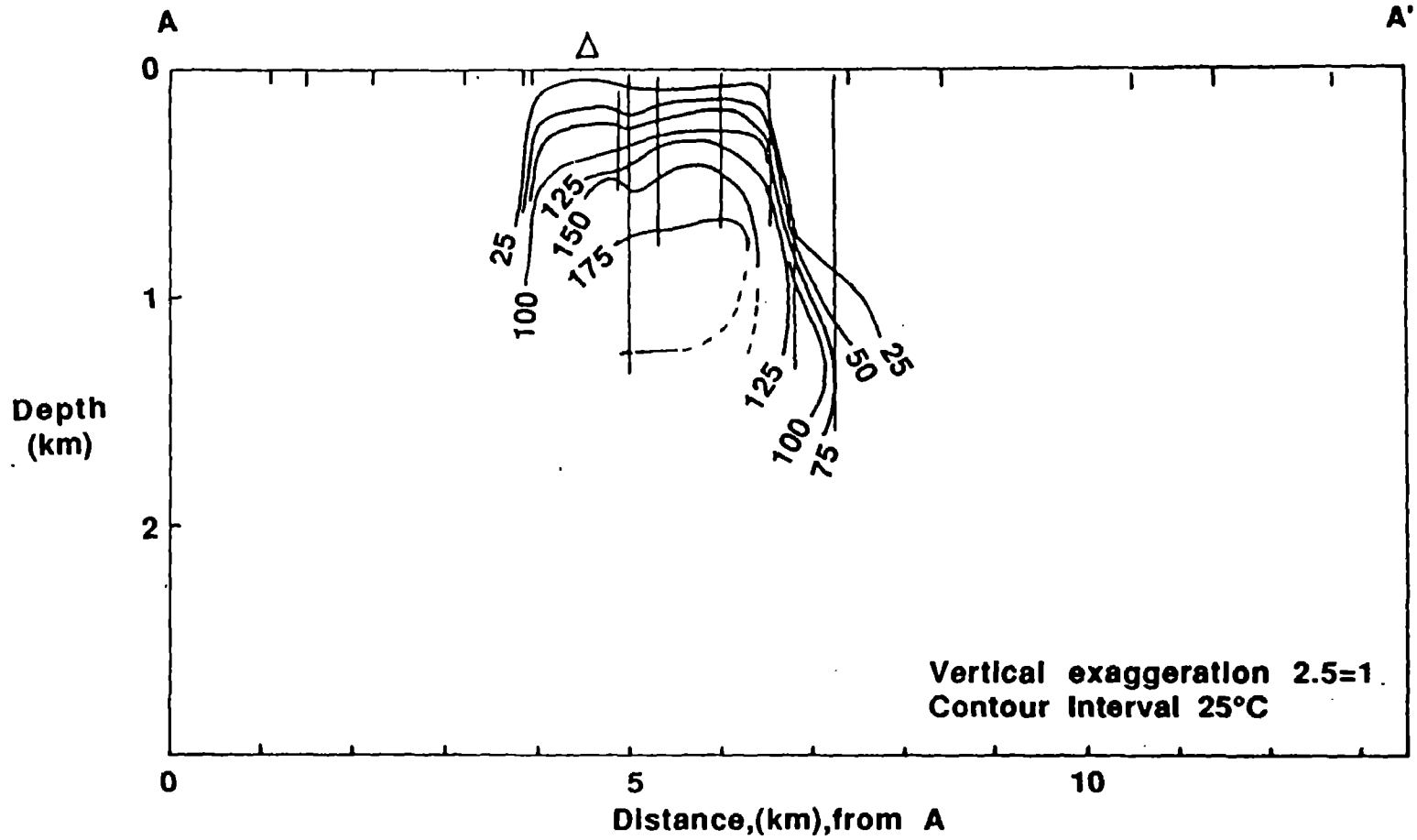

Figure 17A Newmar

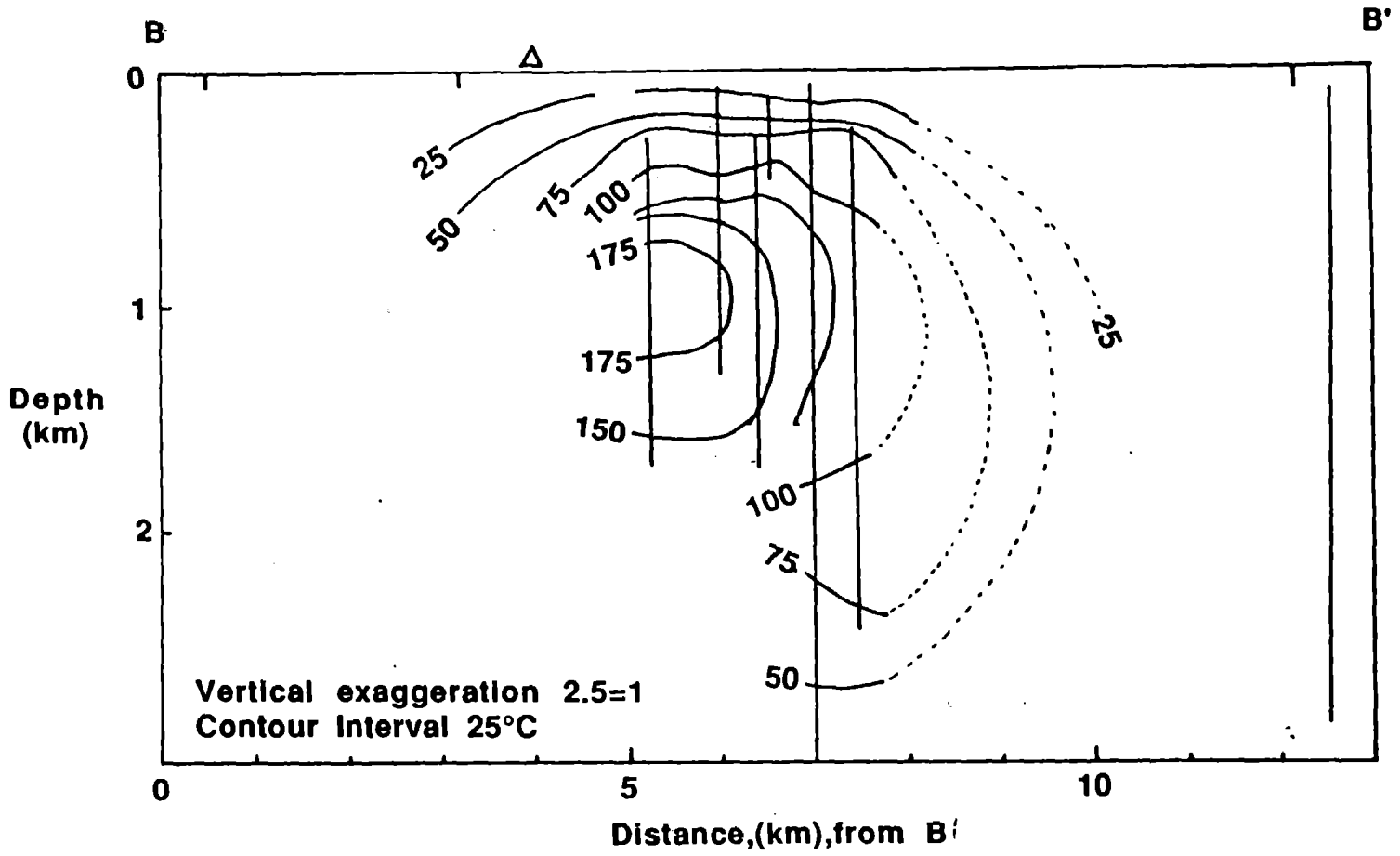

Figure 17b Newmark

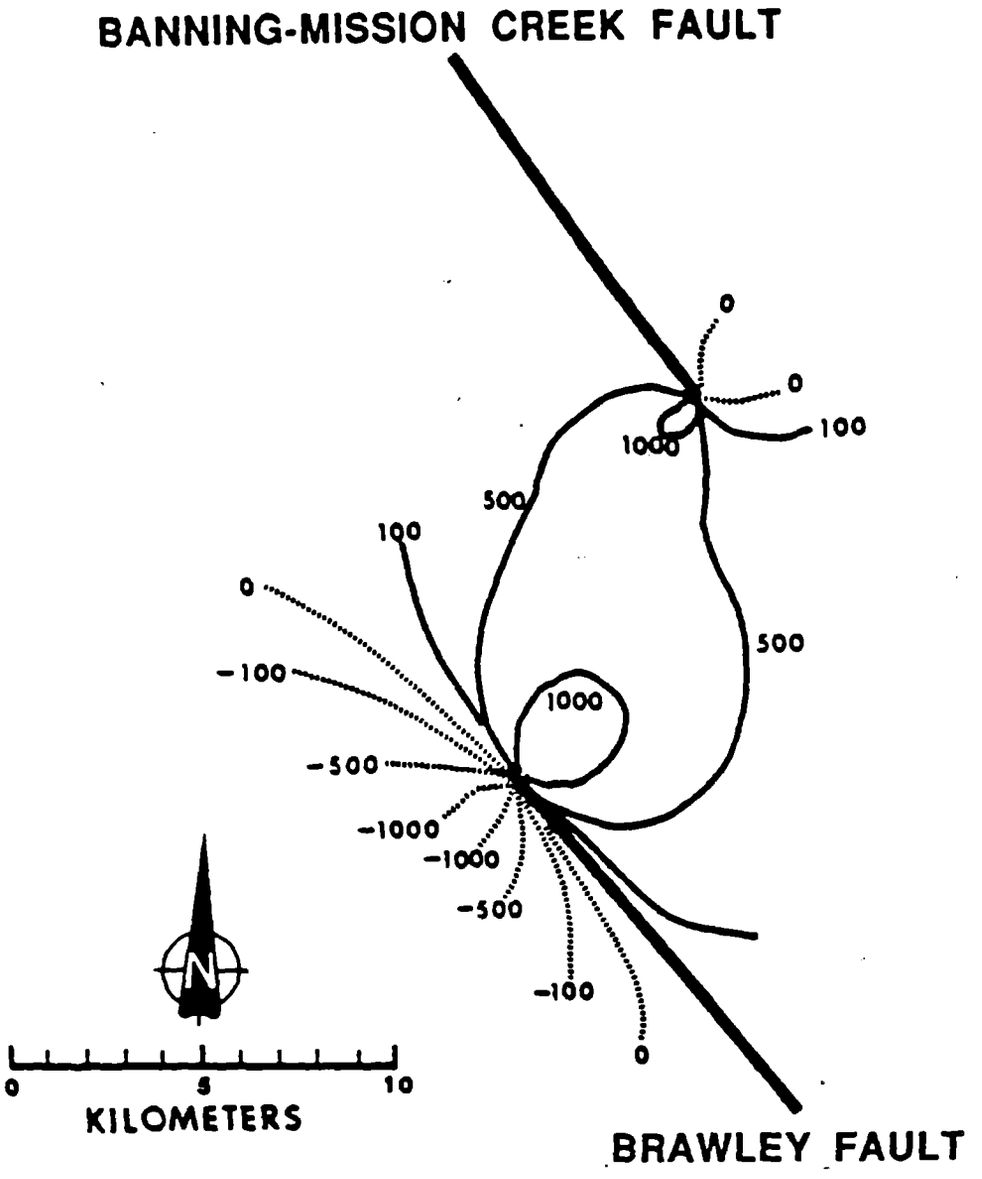

Note: Contour interval is x 10^5 dynes/cm^2.

From Full (1980)

Figure 18 Newmark

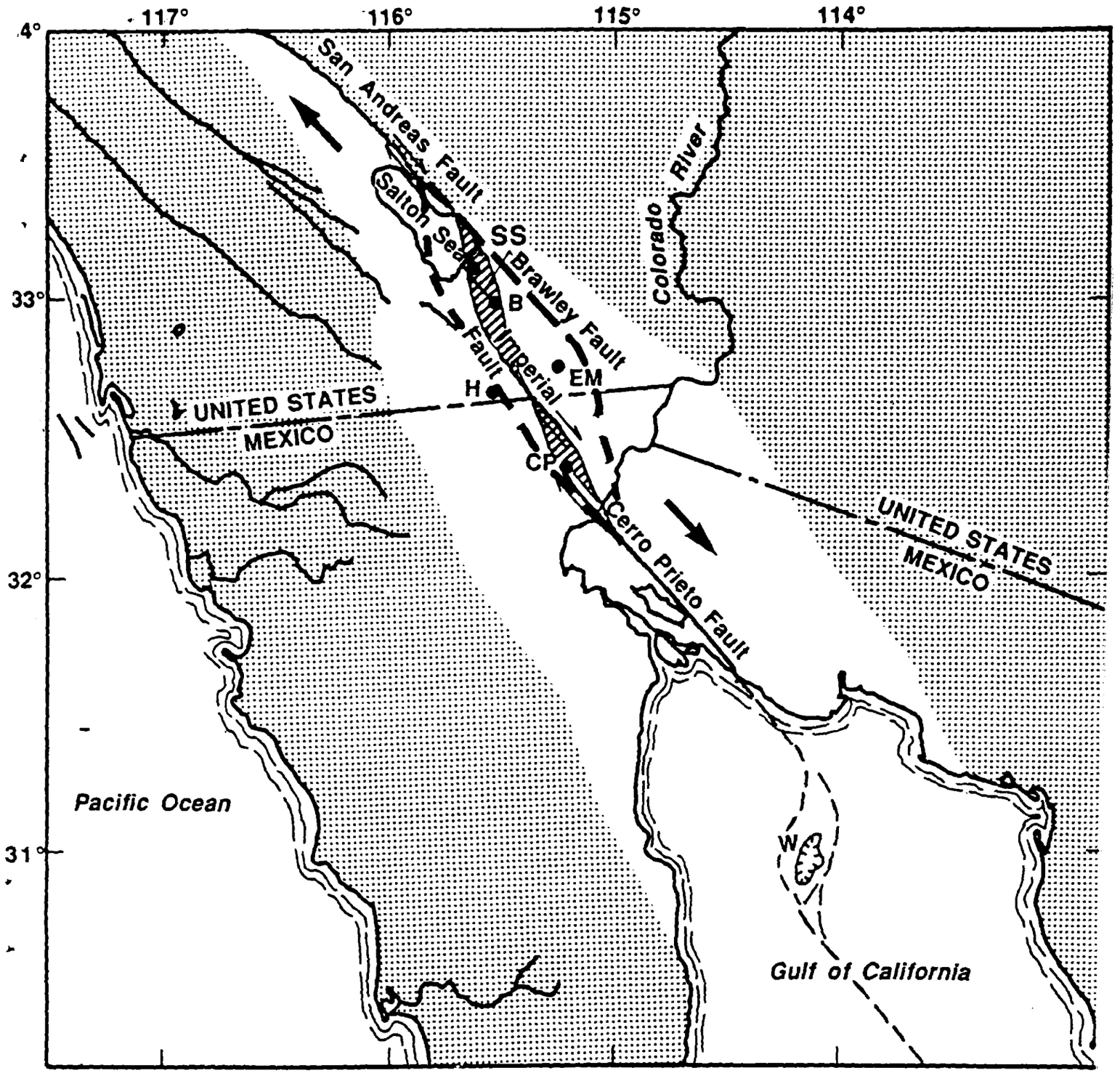

Figure 19 Newmark